Physics – Uspekhi **51** (10) 1027 – 1045 (2008)

METHODOLOGICAL NOTES

PACS numbers: 47.20.Dr, 47.55.nb, 47.55.pf

Certain peculiarities of solutocapillary convection

A L Zuev, K G Kostarev

DOI: 10.1070/PU2008v051n10ABEH006566

Contents

Abstract. **This paper presents experimental results on the solutocapillary Marangoni convection, an effect that occurs in a thin horizontal layer of the inhomogeneous solution of a surface-tension-active agent (surfactant), either near the free upper boundary of the layer or near the surface of an air bubble injected into the fluid. A procedure using interferometry is developed for simultaneously visualizing convective flow structures and concentration fields. A number of new phenomena are observed, including the deformation and rupture of the liquid layer due to a surfactant droplet spread over its surface; bubble self-motion (migration) toward higher surfactant concentrations; self-sustained convective flow oscillations around stationary bubbles in a fluid vertically stratified in concentration; and the existence of a threshold for a solutal Marangoni flow in thin layers. A comparison of solutocapillary and thermo-capillary phenomena is made.**

1. Introduction

1.1 Thermal and solutal Marangoni convection

It is common knowledge that fluids can be set in motion by applying body and surface forces. Among the body forces, the most frequently encountered one is the buoyant (Archimedes) force appearing if the fluid density locally varies in the gravitational field. A fluid parcel that is lighter than the ambient fluid ascends under the influence of the Archimedes force, displacing denser substances downwards. Surface (capillary) forces acting tangent to a free surface or phase boundary of a liquid appear when the surface tension is inhomogeneous and are directed toward the increase [1, 2]. By setting the surface and the adjacent layers of the liquid in motion, these forces trigger the development of a convective flow in the volume, called the Marangoni convection [3] after the Italian scientist Carlo Marangoni, who was among the first at the end of the 19th century to theoretically consider the motion in liquids developing under the action of a surface tension gradient along their free surfaces [4].

In turn, the factors responsible for the formation of an inhomogeneous surface tension σ can vary. The most common and frequently occurring cause is the dependence of σ on temperature. For the majority of single-component organic liquids, the surface tension coefficient decreases linearly as the temperature increases [5]. The ensuing motion is directed along the surface towards a colder region. This is the thermocapillary Marangoni convection. Thermocapillary flows unfailingly accompany nonuniformly heated multiphase systems with interfaces between the phases (or a free surface between a liquid and a gas) and may contribute significantly to heat and mass exchange processes in these systems.

In multi-component liquids, the surface tension can also depend on the chemical composition of the components. In particular, σ is a function of the concentration of the soluble substance in binary solutions. The character of this dependence is determined by the structure and physicochemical properties of the components and most often exhibits a nonlinear behavior [6]. Accordingly, an inhomogeneous

---

A L Zuev, K G Kostarev Institute of Continuous Media Mechanics,
Ural Branch of the Russian Academy of Sciences,
ul. Akad. Koroleva 1, 614013 Perm, Russian Federation
Tel. (7-342) 237 83 14
E-mail: zal@icmm.ru, kostarev@icmm.ru

Received 23 January 2008
Uspekhi Fizicheskikh Nauk **178** (10) 1065 – 1085 (2008)
10.3367/UFNr.0178.200810d.1065
Translated by S D Danilov; edited by A M Semikhatov

distribution of the substance in the solution leads to stresses on its surface, which are analogous to thermocapillary stresses. The result is the development of solutocapillary convection. In this case, flows generated along the surface are directed toward the higher concentration of the surface-active-substance (surfactant). Bearing in mind that the term 'surfactant' embraces several classes of substances [7], we narrow its meaning here to denote the component of the solution that is characterized by the lower surface tension. Correspondingly, its molecules should predominantly accumulate at the free surface of this solution.

Solutocapillary flows play a crucial role in some natural phenomena. One spectacular classical example of the Marangoni convection is given by so-called 'wine tears,' which in some cases spontaneously flow downwards along the inner side of a wine glass filled with a solution of alcohol or other easily evaporating liquid. The mechanism underlying this phenomenon [8] is that with an adequate choice of relevant parameters (the alcohol concentration in the wine, the shape of the glass, the wettability of the inner surface of the glass, etc.), the meniscus part of the liquid, which is in direct contact with the walls of the glass, is depleted of alcohol, because of evaporation, to a greater extent than the rest of the solution. As a result, the solutocapillary forces arising along the surface push the alcohol solution toward the walls of the glass, forcing a thin, practically invisible, liquid film to ascend along the walls against the force of gravity. Having reached the upper edge of the glass, the solution accumulates there, forming a cylinder. The liquid from the cylinder periodically slides down in the form of peculiar droplets ('tears' or 'legs') because of the onset of a Rayleigh – Taylor gravitational instability.

The Marangoni convection essentially influences the intensity of many technological processes common in the food, chemical, oil, and metallurgy industries, including the processes taking place in microgravity, where convective processes mediated by gravity are suppressed or absent. The special attention to research in this area derives from developments in space technology and space life support systems on orbital stations. Thermo- and solutocapillary effects are also important in applications in various branches of science such as ecology (cleaning a water surface of oil contamination), meteorology, hydrology, atmospheric and oceanic physics (evolution of the earth's climate through interactions of the atmosphere with the surface layer of the ocean characterized by significant gradients of the temperature, salinity, and surface active substances dissolved in water [9]), biology (motion of bacteria and cellular organelles), and medicine (propagation of lung surfactant after inhalation of medical aerosols used to cure the respiratory distress syndrome [10]).

1.2 Experimental observation of capillary flows

Despite their frequent occurrence, Marangoni flows are difficult to study experimentally in their pure form. The reason is that the necessary condition for their existence is the presence of temperature or concentration gradients along the surface and, accordingly, in the bulk of liquid. In turn, this inevitably gives rise to local perturbations in density, which is a function of both the temperature and the concentration. As a consequence, the gravitational Rayleigh convection is simultaneously excited in the liquid. Its intensity in terrestrial conditions is frequently found to far exceed, by tens to sometimes a hundred times, that of the Marangoni convection. The latter thus appears to be almost completely suppressed by a more powerful convective mechanism (if directions of capillary and gravitational fluxes are opposite) or masked by its action. It is for this reason that the Marangoni discovery was forgotten for many decades until the second half of the 20th century. Yet, even in the first, now classical publications [2, 3, 11], it was treated as an interesting but rather curios effect promising no important practical applications.

The situation changed dramatically in the 1970s with the advent of the era of technological experiments carried out under conditions of microgravity: in freely falling containers dropped off the top of drop towers, aboard airplanes flying parabolic (Keplerian) trajectories, and in sounding rockets, spacecraft, and orbital stations. The surge of interest in microgravity was first related to the emerging possibility of making materials whose production is hindered by the force of gravity on the Earth [12 – 15]. The conditions under which density contrasts in multicomponent or multiphase media are not accompanied by mass transfer opened up the way to cheap the production of new materials such as alloys of multicomponent metals (solid solutions of homogeneous composition), composites (including foamy materials saturated with air bubbles), quartz glasses with extensive spherical surfaces, large dislocation-free monocrystals for the electronics industry (with a homogeneous distribution of dopants on micro and macro scales), semiconductor materials of high purity, highly homogeneous gel matrices for electrophoresis, and others. By now, hundreds of experiments have already been conducted in space [16 – 20]. Moreover, a separate branch of fluid dynamics has emerged, the microgravity hydrodynamics [21], studying the behavior of liquids in conditions when surface capillary forces significantly exceed body gravitational forces.

But the results of the very first space experiments were discouraging. They proved that even in zero gravity it is impossible to eliminate interfering flows developing in liquids and adversely affecting the homogeneity and quality of the materials obtained. This is partly explained by recognizing that even in the conditions of orbital flight, there remain microaccelerations of different origins caused by vital functions of the crew and functioning of technical systems and equipment, which can reach $10^{-3} - 10^{-4}g$. The amplitude, frequency, and direction of these accelerations are often chaotic and uncontrollable factors, and hence the results obtained in space experiments frequently have a random character and demonstrate poor reproducibility.

There is a more fundamental reason, however. In the absence of gravitational convection, its role is overtaken by capillary convection. The intensity of heat and solutal fluxes mediated by it is more than sufficient to dominate over diffusive processes. The recognition of this fact prompted researchers to revisit the role and implications of capillary phenomena both in zero gravity and on the Earth. The work devoted to this topic is currently exemplified by dozens of monographs and hundreds of articles. But even a cursory glance at this multitude of publications reveals one peculiar feature. The vast majority of the research considers the *thermocapillary* variant of the Marangoni convection, while studies of the *solutocapillary convection* are virtually absent. To a degree, this is due to objective reasons. At first glance, these two phenomena are so alike and almost identical that it seems sufficient to consider only one of them. Indeed, mechanisms underlying the generation of both types of flows are identical (the nonuniformity of surface tension along the liquid surface). The main difference lies only with the *physical* cause of the variations in the surface tension coefficient, whereas the *hydrodynamics* of the problem are largely determined by the presence of a gradient of σ independent of the mechanism generating it. From the theoretical standpoint, equations describing both processes (heat and mass diffusion), as well as boundary conditions, also coincide up to the notation used for variables and coefficients. That is why most of the analytic studies deal with a generalized variant of the problem valid in both cases; the terminology of thermocapillary convection, which is more widely known, is used only to be specific and illustrative.

It is different with the experimental studies. Solutocapillary flows are typically more complex in character and depend on a multitude of various factors, which hamper both their theoretical and numerical analysis and their experimental study. A desire to simplify the problem and remove the complicating side effects is fully reasonable and justifiable. Indeed, in experiments, it is much easier to create, maintain, and measure the gradients of temperature than those of concentration. The lack of simple and adequate methods so far for determining local concentrations of surfactants at the free surface has created the most significant and principal difficulties in studies involving solutal effects. The other difficulty resides in the nonstationary character of solutal flows, which is caused by diffusive processes. While thermocapillary flows are stationary once the temperature contrast is kept fixed, maintaining a steady difference in concentration assumes the presence of sources and sinks of substances at opposite ends of the volume, creating an unwanted extraneous flow. More often it is only possible to maintain a quasistationary concentration gradient, whose magnitude decreases with time due to diffusion. Additional hampering effects related to the solution of a surfactant in the liquid, its evaporation, transformation into a gaseous phase, and absorption at the interface, essentially add to the complexity of the problem [22].

On the other hand, precisely because of this broader variety of acting factors, the solutocapillary flows are of more interest and can be essentially different from thermocapillary flows, despite the similarity of mechanisms supporting them. The main distinction resides in a differing intensity ratio of the diffusive and convective mechanisms of mass transfer, because characteristic times of mass diffusion exceed those of heat diffusion by 2–3 orders of magnitude. As a result, the solutal inhomogeneities persist in a liquid much longer than those due to temperature, while the life time and intensity of the capillary forces at the interface between phases increases manyfold. Furthermore, an additional role is played by the absorption of the surfactant at the interface, which is totally absent in the thermal case. Indeed, the surface of a liquid cannot spontaneously warm up at the expense of cooling in the bulk. This would have led to a reduction in the surface energy, but is prohibited by the laws of thermodynamics. In contrast, the situation where the same interface absorbs molecules of substance with a low surface tension coefficient by extracting them from the solution bulk is rather advantageous energetically and is possible. As a whole, the mechanism of the exit (absorption) of a surfactant at the phase interface is distinct from the mechanism maintaining the temperature at the interface. The interface has inertia, and a convective transfer of the surfactant is possible along it, accompanied by surface diffusion. All these factors contribute to the appearance of new solutocapillary phenomena, which have no thermocapillary analogs.

1.3 Modeling Marangoni phenomena in terrestrial conditions

Experiments conducted directly aboard orbital stations are still rare and rather expensive. Their essential drawback is the necessity of a fully automated experimental procedure and the ensuing limitations, which prevent one from reliably controlling and measuring the full spectrum of the necessary or governing parameters. The lack of the possibility for researchers to operatively intervene in the experiment and modify its goals and technique depending on the situation, as dictated by the results obtained, also hinders fairly complex quantitative investigations. As a consequence, the results obtained in space experiments predominantly carry a qualitative, and sometimes even controversial, character. In these circumstances, the techniques of modeling thermal and solutal Marangoni phenomena in terrestrial conditions acquire a particular status.

As follows from the experimental evidence accumulated up to now [23], the intensity of gravitational convection and other effects related to the action of gravity in terrestrial conditions can be essentially reduced by reducing the characteristic vertical size of the liquid volume. A situation where surface forces are sufficiently strong compared to body forces is realized, for example, in thin layers and films of liquid, liquid bridges, and zones confined between rigid surfaces, and also in small insoluble droplets or bubbles suspended in a liquid. Because the intensity of thermocapillary and thermogravitational convection is respectively governed by the Marangoni and Rayleigh dimensionless numbers [24]

$$\mathrm{Ma}_T = \frac{h^2}{\eta\chi}\,\sigma'_T \nabla T, \qquad \mathrm{Ra} = \frac{\rho g \beta_T h^4}{\eta\chi}\,\nabla T,$$

which characterize the respective ratios of thermocapillary and thermogravitational forces to forces of viscous friction, the prevalence of the thermal capillary mechanism over the gravitational one requires that the quantity

$$\mathrm{Bd} = \frac{\mathrm{Ra}}{\mathrm{Ma}_T} = \frac{\rho g \beta_T h^2}{\sigma'_T}\,,$$

termed the dynamic Bond number, be smaller than unity. This condition bounds the thickness of liquid layers and films (or the vertical size of fluid zones, droplets, and bubbles) eligible for studying thermocapillary phenomena in conditions of normal gravity. For example, the critical thickness $h^* = (\sigma'_T/\rho g \beta_T)^{1/2}$ comprises about 3 mm for ethyl alcohol. In the expressions above, h is the height, $\sigma'_T = \partial\sigma/\partial T$ is the thermal coefficient of surface tension, η is the dynamic viscosity, χ is the thermal conductivity, ρ is the density, β_T is the coefficient of thermal expansion, T is the temperature, and g is the acceleration of gravity.

In solutocapillary problems, the intensity of convection is governed by the diffusion Marangoni number

$$\mathrm{Ma}_C = \frac{h^2}{\eta D}\,\frac{\partial\sigma}{\partial C}\,\nabla C$$

(D is the diffusion coefficient of the surfactant and C is the concentration). Taking into account that diffusion coefficients in liquids are typically lower by 2–3 orders of magnitude than thermal conductivity coefficients and that the solutal coefficient of surface tension $\sigma'_C = \partial\sigma/\partial C$, in contrast, can essentially exceed σ'_T in some solutions and the Marangoni and Prandtl diffusion numbers $\mathrm{Pr}_C = \eta/\rho D$ are commonly much larger than the thermal ones. Therefore, the manifestation of solutocapillary effects can be expected in bodies of liquid with a larger vertical size.

Until recently, research on solutal phenomena was mostly limited to considering the influence of a substance absorbed at the free surface on flows in the liquid. It is known [25] that some long-chain molecules are composed of distinct segments that interact with molecules of the ambient medium in different ways. For instance, hydrocarbon molecules of organic alcohols and fatty acids are composed of polar hydrophilic (water-retentive) and nonpolar hydrophobic (water-repellent) parts. The hydrophobic part reduces solubility in water, and the polar one increases it. Alcohols such as methanol, ethanol, and propanol have short hydrocarbon chains and are fully mixed with water. With an increase in the number of carbon atoms, as is the case with high-molecular-weight alcohols, the solubility decreases and these molecules show a tendency to gather (absorb) at the surface with their hydrophobic part while their hydrophilic ends remain in water. If additionally the surface tension of these solute liquids is smaller than that of the solvent, as is the case with alcohols in water, then by concentrating at the surface, they reduce the surface tension (they are surface-active for it). Water with its high coefficient of surface tension (~ 70 mN m^{-1}) is very sensitive to contamination with surfactants, while substances like silicone oils, whose surface tension coefficient is smaller than 20 mN m^{-1}, can hardly be contaminated.

It suffices for a surfactant absorbed at the surface to form a thin film with a thickness of only one molecule (the so-called Gibbs monolayer [26]). The properties of such monolayers have been studied very thoroughly for a long time [27]. As concerns our problem, it was shown in a set of theoretical [28, 29] and experimental [30 – 34] studies that the presence of a layer of an insoluble surfactant fully suppresses the thermocapillary motion, because it allows compensating thermocapillary stresses at the surface by adjusting the surface density of surfactant molecules and thus creating opposing solutocapillary stresses. That is why ensuring the purity of a liquid surface is an additional complicating prerequisite of thermocapillary experiments, and water is regarded as the least suitable liquid. However, the research literature is virtually void of publications devoted to strictly solutocapillary flows (occurring in the absence of thermocapillary flows) maintained by a given gradient of concentration of the dissolved surfactant. Nevertheless, effects analogous to their thermocapillary counterparts should also be observed in this case.

In this paper, we review experimental results that we obtained in studying the solutocapillary convection developing in thin horizontal layers of liquids in the vicinity of their free surfaces or the surfaces of gas bubbles contained within them. The following tasks have been explored: (1) the deformation and rupture of a thin layer of viscous liquid on a horizontal wettable substrate upon adding a droplet of a soluble surfactant to the free surface layer; (2) the behavior of air bubbles in an inhomogeneous binary solution with a horizontal gradient of the surfactant; (3) a convective flow around resting bubbles in surfactant solutions vertically stratified in concentration. Experimental techniques are described that allow eliminating the hampering gravity effects and visualizing the structure of convective flows and concentration fields in liquids by the interferometry method. Several new phenomena have been discovered, including a solutocapillary migration of gas bubbles in the direction of an increase in the surfactant concentration, self-oscillatory regimes of solutal convection in a vertical gradient of the surfactant, and the threshold character of excitation of solutocapillary flows near the free surface.

2. Rupture of a liquid layer by a solutocapillary flow

2.1 Thermocapillary deformation of a liquid layer

Thermocapillary flows in thin horizontal liquid layers with free upper surfaces and lateral temperature gradients have been well explored to date. It follows from numerous analytic solutions (see, e.g., [11, 35 – 37]) that the condition of constant pressure at the free surface of such layers cannot be satisfied without changing their thickness. The emergence of thermocapillary convection is accompanied by a change in normal stresses, and the equilibrium shape of the surface is therefore deformed. An equation for the free surface shape is derived in [37] in an approximation analogous to the boundary-layer approach. It is shown that as the thickness of the layer decreases, the deformation of the surface increases profoundly and becomes comparable to the thickness proper. This finds support in the results of an experimental study dealing with a thermocapillary deformation of a thin liquid layer located at a rigid wettable substrate rectangular in shape and characterized by a linear temperature distribution. Appreciable deformation has only been observed in liquid layers thinner than 1 mm. The deformation reached the bottom of the cell if the temperature gradients were sufficiently large. The conditions of layer rupture through the thermocapillary flow were experimentally explored in Ref. [38]. The minimum temperature difference necessary for the rupture proved to be proportional to the layer thickness squared, which agrees well with calculations in Ref. [37] performed in the case where the spatial period of temperature modulation was large compared to the capillary constant. For example, given a layer of n-decane with the thickness 0.5 mm, the critical temperature contrast ΔT^* between the heated and cooled ends of the layer comprised 20 °C, while for a 0.7 mm layer, it was already 40 °C.

A similar problem for axisymmetric geometry was experimentally explored in Ref. [39]. A liquid layer with a thickness up to 2 mm was created in a cell of a cylindrical shape (∅ 90 mm) heated in the center and cooled along the periphery. A stationary radial flow developed in the layer. Its direction near the surface was toward the higher surface tension area, i.e., to the periphery of the cell, with a returning flow headed to the center along the cell bottom. The experiments were carried out with several organic liquids of various viscosities (n-decane, n-heptane, ethanol). In all cases, the development of the flow caused a local deformation of the layer surface with the thickness decreasing substantially over the heater. The deformation amplitude increased on reducing the initial layer thickness or increasing the temperature contrast between the center of the cell and cold parts of the surface close to the periphery. Beginning from a certain contrast magnitude ΔT^*, a dry zone formed over the heater. Its radius also increased together with the temperature contrast. The liquid receded, exposing a part of the cell bottom, with the dynamical contact angle being different from zero even for highly wetting liquids. The maximum thickness of the layer undergoing the rupture turned out to exceed that of the layer in the rectangular cell by a factor of 1.5.

2.2 Solutocapillary deformation of a liquid layer

Our first experiments [40, 41] devoted to studies of layer deformations caused by a solutocapillary Marangoni flow indicated that deformations similar to those in the thermocapillary case also occur in the presence of surfactants on the free surface. This even happens for much thicker layers, because it is possible to achieve much larger surface tension gradients in this case. Similar phenomena have been observed in some technological processes. For instance, Ref. [42] describes the growth of a monocrystal on a substrate, in a thin horizontal layer of an aqueous solution of the salt $Ba(NO_3)_2$ on a glass plate under isothermal conditions. As water evaporates from the free surface, the solution becomes oversaturated, and a crystal in the shape of a thin needle begins growing in it. The authors discovered that the surface of this solution oscillates. The liquid periodically withdraws from the crystal, leaving it to lie on the dry glass, and then returns, bathing the crystal. During these retreats, the growth of the crystal was apparently halted, and hence the crystal was acquiring not a homogeneous but a wavy structure. This behavior of the solution can be explained by precisely the development of solutocapillary convective motion: because the surface tension of the aqueous solution of $Ba(NO_3)_2$ is proportional to its concentration, it decreases as the crystal starts growing because of local depletion of the salt in the solution. A Marangoni flow is generated along the surface of the solution in the direction from the crystal, causing the surface deformation and retreat of the liquid phase. As soon as the liquid is withdrawn from the crystal, the depletion of the salt in the solution is immediately terminated, diffusion restores the homogeneity of the concentration, the Marangoni convection is extinguished, and the liquid returns.

The task about the response of a liquid layer to small amounts of the surfactant deposited at its surface has important implications for various branches of technology. But the analysis of publications shows that the majority of them, predominantly theoretical ones, do not focus on conditions of solutocapillary deformation and rupture of liquid layers, but instead deal with determining the speed of the spread of a monolayer of an insoluble surfactant over a free surface. A thorough review of the literature related to this question is given in Ref. [43].

Analytic results [44, 45] indicate that the developing shear flow noticeably deforms the surface under the condition that gravity effects are negligibly small (for a layer 1 – 2 mm thick). Ahead of the propagating surfactant front, a characteristic elevation of the surface (crest) develops, followed by a reduced layer thickness behind the propagating front. Papers [46, 47] demonstrate that the same phenomenon is also observed in the case of a soluble surfactant. The account for diffusion of the surfactant across the layer shows that the desorption caused by the surfactant solution in the bulk of the liquid reduces the propagation speed compared to the case of an insoluble surfactant, and yet the deformation of the surface becomes even stronger. The system of equations obtained in these works also describes a Marangoni flow caused by a heated spot on the surface [47]. In numerical simulations, the maximum height of the crest reached the doubled thickness of the unperturbed layer, whereas the minimum thickness did not drop below 1/10 of it. Meanwhile, it was observed in experiments [48 – 50] that soon after placing a drop of an insoluble surfactant on the surface of a layer 0.3 – 0.4 mm thick, the deformation continued all the way to the rupture of the layer, and a dry spot formed on the bottom. This cannot be explained in the framework of the theory referred to above. For the sake of fairness, we note that in all the experiments, relatively large drops ($\sim$ 30 μl) were placed on the surface, such that the amount of surfactant needed to build a monolayer was exceeded manyfold. We did not succeed in finding other experimental works devoted to the dynamics and conditions of solutocapillary layer rupture in the current literature.

2.3 Experimental technique

In our experiments [51, 52], we used drops of liquid with the surface tension smaller than that of the liquid in the layer. Being placed on the layer surface, such drops first tend to spread in a spot of minimum thickness and maximum size, i.e., within a monomolecular film, which then quickly disappears in the process of evaporation or solution. Because the distribution of the surfactant over the surface is nonstationary, the layer deformation responds accordingly. In such circumstances, for comparison with the thermocapillary case, we have to measure the parameters of maximum deformation, specifically the radius r of the forming dry spot and the critical layer thickness h^* at which the layer undergoes a rupture. The external parameters in experiments were the initial thickness h_0 of the unperturbed liquid layer, the volume V of the introduced surfactant, and the difference of surface tension coefficients $\Delta\sigma$, which was varied by selecting different pairs of mixing liquids. In this way, it was possible to proceed without direct measurements of the surfactant concentration at the surface.

Isopropyl alcohol was used as the surfactant in one series of experiments, and distilled water or an aqueous solution of isopropyl alcohol were used as the layer-substrate. In other cases, the substrate layer was of tridecane and the drops were of isopropyl alcohol or hydrocarbons with a smaller surface tension (hexane, heptane, decane, undecane, cyclohexane). Tables 1 and 2 list the surface tension coefficients of the liquids used [53]. For example, hexane and heptane are surfactants for isopropyl alcohol, which, in turn, is a surfactant for the rest of the hydrocarbons.

The experiments were conducted as follows. To create a thin horizontal layer 0.1 to 3 mm in height, the chosen working liquid with a volume of 1 – 20 cm^3 was poured into a glass cell having the form of a shallow vertical cylinder (a Petri dish). The cell was arranged on an electronic balance

Table 1. Surface tension coefficients of liquid pairs used in experiments.

Base layer		Surfactant droplet		$\Delta\sigma$, 10^{-3} N m^{-1}
Liquid	σ, 10^{-3} N m^{-1}	Liquid	σ, 10^{-3} N m^{-1}	
Isopropanol	21.22	n-Hexane n-Heptane	17.93 20.06	3.29 1.16
n-Tridecane	25.04	Isopropanol n-Hexane n-Heptane n-Decane Cyclohexane	21.22 17.93 20.06 23.43 24.35	3.82 7.11 4.98 1.61 0.69

Table 2. Surface tension coefficients in aqueous solutions of isopropanol.

Base layer		Surfactant droplet		
Concentration C_0, %	σ, 10^{-3} N m^{-1}	Liquid	σ, 10^{-3} N m^{-1}	$\Delta\sigma$, 10^{-3} N m^{-1}
0	72.20	Isopropanol	21.22	50.98
5	56.22			35.00
10	40.42			19.20
15	35.50			14.28
20	30.57			9.35
25	28.70			7.48
30	26.82			5.60
35	26.05			4.83
40	25.27			4.05
45	24.77			3.55
50	24.26			3.04
55	23.89			2.67
60	23.51			2.29
65	23.10			1.88
70	22.68			1.46
75	22.41			1.19
80	22.14			0.92
85	21.92			0.70
90	21.69			0.47
95	21.46			0.24

ensuring a mass measurement accuracy of 0.01 g, which allowed the layer thickness to be controlled with an error of 0.01 mm. The required amount of the surfactant was introduced as a drop at the center of the layer surface through a volumetric pipette, which delivered volumes ranging from 0.5 to 55 µl. The entire process was recorded with a videocamera at 25 frames per second. The experiments were carried out at the constant ambient temperature 25 ± 1 °C.

2.4 Conditions of layer rupture

Placing a drop of a soluble surfactant on the surface of the layer in the center of the cell led to a local reduction in the surface tension accompanied by the appearance of radially directed solutocapillary Marangoni forces proportional to the difference of surface tension coefficients of the pair of liquids used. Driven by these forces, the deposited surfactant tended to quickly spread to the cell periphery, reaching it in fractions of a second (the photograph in Fig. 1a shows a spreading hexane spot 0.3 s after placing the drop on the surface of an isopropyl alcohol layer). This flow, in turn, entrained subsurface layers of the substrate liquid, enforcing a local reduction in the thickness of the layer under the surfactant spot. As the spot area increased, the surface concentration of the surfactant decreased and, as a consequence, the surface tension gradients and the spreading speed of the surfactant also decreased. If the initial thickness of the liquid layer was sufficiently large, the deformation soon disappeared (within 1 – 2 s). In thinner layers, the developing depression reached the cell bottom, exposing a part of it. The size of the developing dry axisymmetric zone appeared to be much smaller than the size of the spreading surfactant spot, while the contact angle of the liquid touching the rigid surface differed from zero, as in the case of thermocapillary deformation [39]. The diameter of the dry zone first increased, reaching a maximum at some instant (Fig. 1b) and subsequently decreasing (Fig. 1c) as the surfactant dissolved.

As was revealed by the measurements, the diameter of the rupture was determined to a large extent by the thickness of the layer, the amount of the surfactant introduced onto the surface, and the difference of surface tension coefficients. The thinner the liquid layer was, the larger the rupture and the longer its lifetime (in some cases, up to several minutes) were. Figure 2 shows plots of the dependence of the maximal radius of the dry zone on the initial thickness of an isopropanol layer for fixed-size hexane drops deposited on the surface of the layer. Experimental points, each obtained by averaging over several realizations, are fairly well approximated by polynomial fits. The error in measuring the rupture radius, which is not shown in the plots, did not exceed 5 – 10%, being maximal in the range of small thicknesses (large rupture radii) when the emerging dry zone was already losing its concentric shape. These results allowed determining the critical layer thickness h^* for which the deformation of the surface coincides with the layer thickness and the radius of the dry zone reduces to zero. It turned out that although the rupture radius increased with an increase in the amount of the surfactant, the critical layer thickness was independent of the surfactant volume (curves *1* – *3*). Such a behavior of h^* is most likely explained by the fact that the amount of the surfactant used in experiments was much larger than that needed to just enforce the rupture. For the liquid pair hexane – isopropanol, h^* was ~ 1.2 mm. We note that in subsequent experiments conducted with isopropyl alcohol drops of various concentrations deposited on a water layer surface, the critical layer thickness showed no dependence on the content of the isopropanol in the drops.

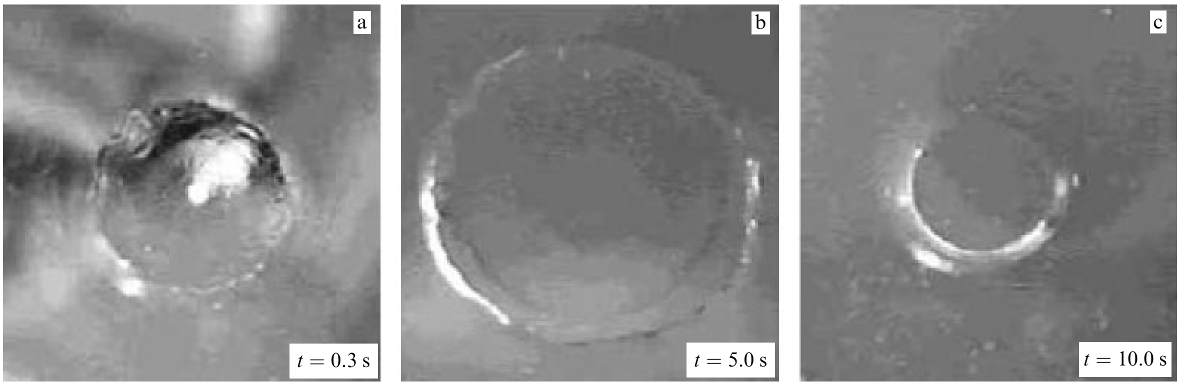

Figure 1. Evolution of the deformation caused by a hexane drop placed on the surface of an isopropyl alcohol layer (a view from above). The initial layer thickness $h_0 = 0.7$ mm.

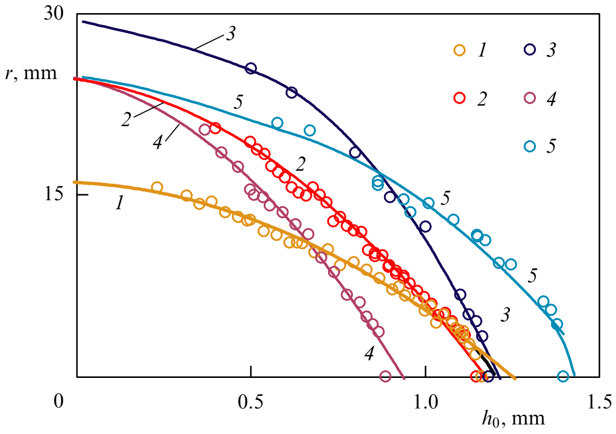

Figure 2. Dependence of the maximum radius of the dry zone on the initial layer thickness: *1–3*, the hexane–isopropanol pair, drop volume $V = 10$ μl (*1*), 20 μl (*2*), 50 μl (*3*); *4*, the heptane–isopropanol pair, $V = 20$ μl; *5*, isopropanol–tridecane, $V = 20$ μl.

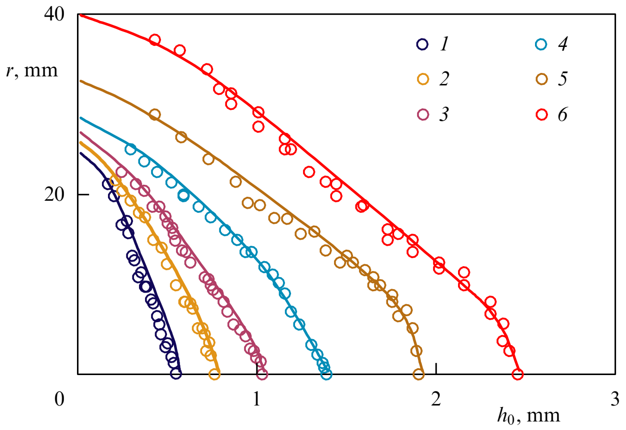

Figure 3. Dependence of the maximum radius of the dry zone on the initial layer thickness for an isopropanol–isopropanol pair solution. The initial alcohol concentration C_0 in the solution: 90% (*1*), 75% (*2*), 50% (*3*), 25% (*4*), 10% (*5*), and 0% (*6*).

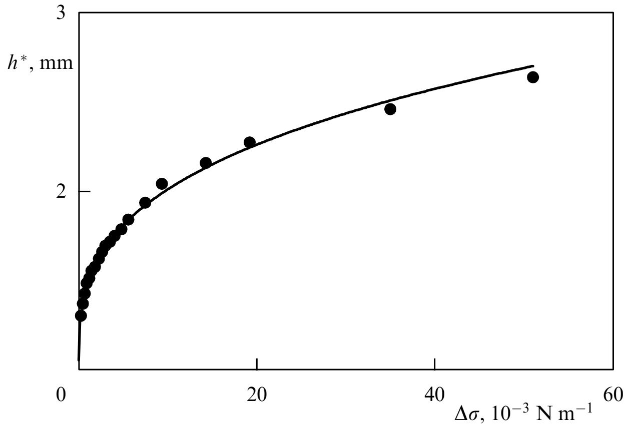

Figure 4. Dependence of the critical layer thickness on the difference of surface tensions of the liquids in the drop and in the layer (isopropanol–aqueous solutions of isopropanol)
.

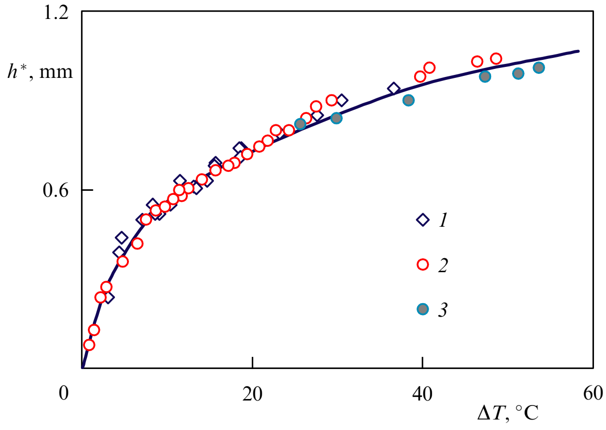

Figure 5. Dependence of the critical layer thickness on the temperature difference: decane (*1*), heptane (*2*), and ethanol (*3*).

Curves *2*, *4*, and *5* in Fig. 2 plot dependences of the maximum rupture radius on the layer thickness for three pairs of drop–substrate liquids (heptane–isopropanol, hexane–isopropanol, and isopropanol–tridecane) differing in the surface tension contrast $\Delta\sigma$ (1.16, 3.29, and 3.82 mN m^{-1}, respectively). As can be seen from the plots, the critical thickness of the layer and the size of the rupture increase as $\Delta\sigma$ and the intensity of solutocapillary flow increase. Moreover, experiments conducted in cells of various diameters proved that both the radius of the developing dry zone and the critical thickness are virtually independent of the horizontal layer size (at least for $r \geqslant 10$ mm). The error in measurements of h^* in these cases did not exceed 0.01 mm. The dependence of the rupture zone size on the surfactant drop volume has the simplest shape. It turned out that the radius squared of the dry zone (i.e., in fact, its area) is linearly proportional to the volume of the drop.

The dependence of h^* on the difference of surface tensions was explored in a set of experiments in which drops of pure isopropanol were placed on surfaces of its aqueous solutions of various concentrations. This permitted obtaining rather large surface tension differences, $\Delta\sigma \sim 50$ mN m^{-1} (see Table 2). Figure 3 displays the dependences of the maximum rupture radius on the thickness of the solution layer for a set of isopropanol concentrations. We see that the rupture of the surface in this case already occurs for noticeably thicker liquid layers reaching 2.5 mm. As the concentration of the isopropanol in the solution increases (and, accordingly, the surface tension of the solution decreases), the critical layer thickness decreases. This effect is particularly apparent in the region of small concentrations because of the strongly nonlinear dependence of the surface tension coefficient on the alcohol concentration. The dependence of the critical thickness on the respective difference of surface tensions of the drop and the solution is presented in Fig. 4. The experimental data are approximated reasonably well by a logarithmic curve.

We note that a similar behavior is displayed by the dependence of the critical layer thickness on the temperature difference plotted in accordance with the results of measurements carried out in Ref. [39] (Fig. 5). To facilitate comparison of rupture conditions for solutal and thermal Marangoni convections, all the experimental data are summarized in Fig. 6. Because the difference in surface tensions spans a much larger range of magnitude in the solutal case than in the thermocapillary one, the values along the abscissa are plotted

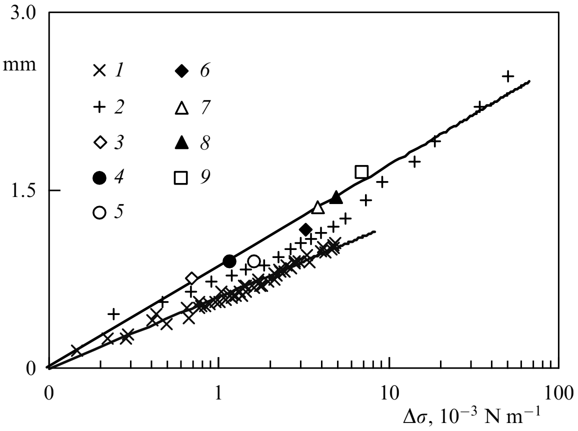

Figure 6. Dependence of the critical layer thickness on the difference of surface tension coefficients: *1*, thermocapillary convection and *2–9*, solutocapillary convection. Pairs of liquids: aqueous solutions of isopropanol (*2*), cyclohexane – tridecane (*3*), heptane – isopropanol (*4*), decane – tridecane (*5*), hexane – isopropanol (*6*), isopropanol – tridecane (*7*), heptane – tridecane (*8*), hexane – tridecane (*9*).

in a logarithmic scale. This same plot also shows the experimental points obtained with hexane and heptane drops put on the surface of isopropyl alcohol, and hexane, heptane, decane, and with cyclohexane drops put on the surface of tridecane. The comparison demonstrates good agreement between thermal and solutal dependences of the critical thickness on the difference of surface tensions. As can be noticed, the experimental points related to all situations are grouped in one domain. Somewhat lower values of the critical thickness for a thermocapillary rupture compared to a solutal one (about 30%) are most likely the consequence of the fact that in the experiment in [39], the temperature of warm and cold regions was measured with thermocouples pressed into the cell bottom, whereas the actual temperature contrasts could be lower on the surface of the layer owing to heat emission. Thus, the results obtained in experiments give evidence that the layer thickness starting from which the rupture occurs is practically independent of the physicochemical properties of the liquid itself (first and foremost, the properties like density and viscosity), as well as of the way the surface tension contrast is created on the surface (thermal or solutal), but is largely determined by the magnitude of this contrast.

3. Solutocapillary migration of air bubbles

3.1 Thermocapillary migration of air bubbles

The ability of gas bubbles (or insoluble drops) suspended in a nonuniformly heated liquid to self-propel toward a warmer region as if they were attracted to the heat source was first discovered in Ref. [54] and was called the *thermocapillary migration*. In Russian literature, the term *thermocapillary drift* emerged later [55]. The motion is caused by tangent thermocapillary forces occurring at the surface of the bubble. They induce the liquid surrounding the bubble to flow past it along the surface tension gradient from the warm to the cold pole. As a result, a net reaction force is exerted on the bubble and pushes it in the opposite direction. The phenomenon of thermocapillary migration is presently well explored. The most detailed reviews of theoretical and experimental works devoted to the topic can be found in monographs [56 – 59]. As follows from theoretical estimates [54, 55], the speed of thermocapillary migration is constant in a uniform temperature gradient at small Marangoni and Reynolds numbers (the creeping flow approximation) and proportional to the surface tension gradient and the size of the bubble, and inversely proportional to the viscosity of the liquid. As an example, the speed of a bubble 1 mm in diameter can reach several centimeters per second in the temperature gradient 1 K cm^{-1}, depending on the properties of the surrounding liquid. Given this value of speed, the thermocapillary migration acquires practical importance for a large number of various technological processes that deal with gas inclusions under nonisothermal conditions.

Although the thermocapillary migration was theoretically predicted relatively long ago, the process of its experimental confirmation took many years. The principal difficulty comes from the need to separate the thermocapillary and gravitational contributions to the velocity. The gravitational contribution comes from the vertical floating of a bubble under the action of Archimedes forces and can often exceed the thermocapillary migration velocity by an order of magnitude. In terrestrial conditions, it is also fairly difficult to isolate the bubble entrainment by convective currents unavoidably emerging in the ambient fluid if it is nonhomogeneously heated. The magnitude and direction of such transport are strongly variable and depend on the location of the bubble. This requires creating approaches and techniques for minimizing the gravitational motion of bubbles (for example, by conducting experiments in zero gravity) or reliably discriminating thermocapillary migration against a background of interfering effects.

On the Earth, the most widespread way of studying the thermocapillary migration, first used in [54] and further elaborated in Refs [60, 61], consists in placing an air bubble in a volume of liquid heated from below. The basic idea of this approach exploits the fact that the speed of thermocapillary motion of the bubble is linearly proportional to its size (the radius R), while the speed of Archimedes surfacing is proportional to R^2. Thus, for sufficiently small bubbles, the balance is possible between the Archimedes and thermocapillary forces directed, respectively, upward and downward, such that the bubbles can hover motionless in the liquid or even sink if heating is increased. The temperature gradients measured in such experiments were in good agreement with theoretical estimates. An essential drawback of this approach is that its applicability is limited to very small bubbles (with the radius 100 – 200 µm) and to small temperature gradients and sufficiently large viscosities of working liquids to remain below the critical Rayleigh number and avoid the onset of gravitational convection. Moreover, only the magnitude of the thermocapillary force exerted on the bubble is actually determined in such experiments, whereas observing the direct migration and measuring its velocity remains impossible.

We have proposed a technique to study the thermocapillary migration of bubbles in thin horizontal liquid layers with a lateral temperature difference [63, 62]. A mutually perpendicular orientation of the temperature gradient and the force of gravity allows differentiating between the horizontal (thermocapillary) and vertical (gravitational) components of the bubble velocity. Because the upper rigid boundary of the layer limits the vertical motion of a bubble pressed to the surface by Archimedes forces, the bubble can only move horizontally in the direction of the temperature gradient. The shallowness of the liquid layer ($\sim$ 2 mm) drastically reduced the intensity of the gravitational convection caused by the temperature differences, and hence characteristic velocities of convective motion were essentially smaller than the velocity of the bubble motion. Small air bubbles with a diameter less than the layer thickness remained spherical when injected into the layer, while large bubbles took the form of a cylindrical tablet flattened out by the horizontal walls of the layer. Admittedly, for bubbles of such a shape, their interaction with the rigid boundaries of the layer played a significant role. A necessary condition for the free motion of a bubble was the presence of a thin separating layer between its butt-ends and the walls. Its existence was confirmed by interferometric observations. The motion of bubbles was recorded by a videocamera through the upper glass plate. In the course of experiments, speeds of thermocapillary migration were measured as functions of time, the temperature gradient, the shape and size of bubbles, and the thickness of the liquid layer for several organic liquids (methanol, ethanol, heptane, decane). The results obtained in experiments qualitatively agree with the analytic results in Refs [54, 55], although the value of the migration speed is quantitatively an order of magnitude lower than that for a freely moving bubble in a three-dimensional volume of liquid.

3.2 Observation of solutocapillary migration of bubbles

It is reasonable to assume that given a surfactant solution of inhomogeneous composition, a similar, solutocapillary migration of gas bubbles may exist, being directed toward higher concentrations of the surface-active component of the solution. This type of behavior was observed for gas inclusions in some processes in technology, particularly in casting. It is known that in continuous casting, for example, of molten steels, the defects related to the presence of bubbles have a detrimental effect on the quality of ingots and must be avoided to the maximum possible degree. In this vein, gas bubbles expelled by a crystallization front during crystallization of some substances from their aqueous solutions cooled from below were investigated in [64]. It was discovered that sufficiently small bubbles located in the solution in close proximity to the crystallization front moved downward against the Archimedes force (sank). The explanation of this behavior of bubbles cannot be the thermocapillary migration because for a temperature gradient directed upward, the direction of migration would be just the opposite to the observed one. The authors hypothesized that a boundary layer forms ahead of the front, in which, besides the temperature gradient, a gradient of concentration of various dissolved surfactants also arises, forcing the bubbles to sink. They also suggested a theoretical model for such motion [65].

To explore this phenomenon in more detail, a special experiment was designed [66]. The behavior of bubbles rising in a close vicinity to the vertical surface of freezing water was investigated for various freezing conditions and physicochemical properties of components added to water. Aqueous solutions of NaCl (the dependence of their surface tension on the concentration is so small that they can be considered virtually surface-inactive for the surface of water) with concentrations $1.05-11.3$ mol m^{-3} and an aqueous solution of the surface-active reagent $C_8H_{17}SO_3Na$ with concentrations $0.185-0.85$ mol m^{-3} were used in the experiments. To maximally suppress the intensity of free convection, the solution was confined in a narrow gap (only 0.65 mm thick) between two vertical glass plates of dimensions $30 \times 20 \times 1$ mm, one of which was cooled to $-20\,°$C. In this way, a vertical crystallization front was created that propagated horizontally at the speed about 5 μm s^{-1}. Small hydrogen bubbles (up to 30 μm in radius) were created in the water solution through electrolysis. Independent methods were applied to measure the temperature (thermocouple measurements) and solution concentration (emission spectrophotometry), and also the coefficient of surface tension, the coefficient of surfactant diffusion in water, and the equilibrium coefficient of surfactant distribution between water and ice. The behavior of bubbles was recorded with a videocamera, and the diameter of bubbles and their distance from the ice front was determined directly from video stills.

It was found that in NaCl solutions far from the crystallization front, all bubbles floated strictly upward. But in the solution of $C_8H_{17}SO_3Na$, bubbles located closer than 150 μm to the front showed very fast horizontal displacement to the front and were then trapped by it. The fact that such a behavior occurred only in the surfactant solution provides grounds to argue that the solutocapillary migration was observed. The authors carefully estimated the feasibility of other factors contributing to the horizontal bubble displacement, including gravitational convection, thermocapillary migration, and the presence of a pressure gradient caused by a difference in the velocities of the flow around the bubble at the bubble sides (the Saffman effect [67]), and firmly established that their influence is small compared to the effect of the surfactant concentration gradient. Experimental dependences of bubble solutocapillary velocities were obtained as functions of the bubble radius, the initial surfactant concentration in the solution, and the crystallization rate. They agree well with the theoretical predictions in [65]. But because the direct measurement of the concentration gradient in the boundary layer turned out to be impossible (in that work, it was estimated only empirically, based on the mean observed boundary layer thickness, taken as 90 μm, the initial solution concentration, and the measured diffusivity coefficients), the dependence of the migration speed on the concentration gradient remained unexplored.

3.3 Experimental technique

The method used in our experiment [68 – 70] to neutralize the action of the forces of gravity is analogous to the method applied earlier to study thermocapillary migration of bubbles in an inhomogeneously heated liquid [62, 63]. Small air bubbles were injected into a thin horizontal liquid layer with a lateral concentration gradient. Maintaining a stationary contrast in concentrations requires supplying an enriched solution and, consequently, creates a forced flow, and we therefore had to use a quasistationary gradient, whose magnitude decayed with time because of diffusion. This required continuous monitoring of the surfactant concentration with optical means (interferometry). The experimental cuvette was an interferometric cell arranged horizontally. It had a thin (1.2 mm in thickness) cavity with a rectangular base 90×40 mm and plane-parallel glass walls with a semitransparent reflecting coating. The observations were made from above (from the side of large faces) in the reflected light. To visualize the distribution of the surfactant concentration in the cavity, we used a laser Fizeau interferometer [71]. In the isothermal case, the interferometer allowed visualizing anomalies in the solution concentration as a set of fringes representing bands of equal optical paths. If the solution composition changes only perpendicular to the sounding light

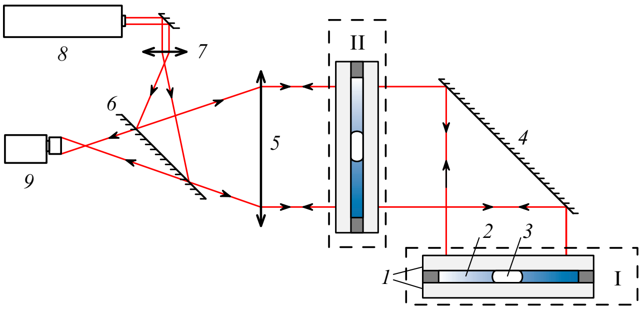

Figure 7. Schematics of the experimental setup: *1*, glass plates with a semitransparent reflecting coating; *2*, the liquid layer; *3*, the air bubble; *4*, mirror; *5*, lenses; *6*, semitransparent mirror; *7*, microlenses; *8*, He–Ne laser; *9*, videocamera. I and II are positions of the cell in horizontal and vertical orientation.

beam, as in our case, each interference fringe can be identified with a certain surfactant concentration value, based on the concentration dependence of the refractive index. For a layer 1.2 mm thick, the transition from one monotonous interference fringe to another corresponds, on average, to a 0.3% anomaly in the concentration of an aqueous alcohol solution. The experimental setup is sketched in Fig. 7.

The cavity was filled with an inhomogeneous mixture of two miscible liquids with different surface tension coefficients. Aqueous solutions of methyl alcohol with concentrations C_0 between 80 and 100% were used (the concentration is the mass fraction of the surfactant dissolved in water). The choice of methanol solutions as working liquids was motivated by preliminary experiments with various mixtures. These experiments indicated that for the majority of liquids, the arising solutocapillary flows are too weak to overcome the frictional forces of bubbles against the walls and set the bubbles in motion. In experiments with methanol solutions, the solutocapillary bubble migration was reliably observed owing to the optimum combination of physicochemical properties of this alcohol. Besides meeting basic requirements imposed on working liquids (full wettability, transparency, nonaggressive character, density close to that of water), methyl alcohol has the minimum viscosity and surface tension [6]. This makes it the strongest surfactant with respect to water. In conjunction with the low viscosity, this considerably enhances the intensity of solutocapillary flows. Over the selected range of concentrations, methanol solutions offer a nearly linear dependence of the density, viscosity, surface tension, and refractive index on the concentration. All experiments were carried out in an isothermal regime at the ambient temperature 20 ± 1 °C.

A lateral concentration gradient was created in the horizontal solution layer by the following technique. First, the experimental cell was arranged vertically, with a small face as a base. It was half-filled with a methyl alcohol solution with the concentration 80–90% (the corresponding interference pattern is given in Fig. 8a), and then a lighter, pure

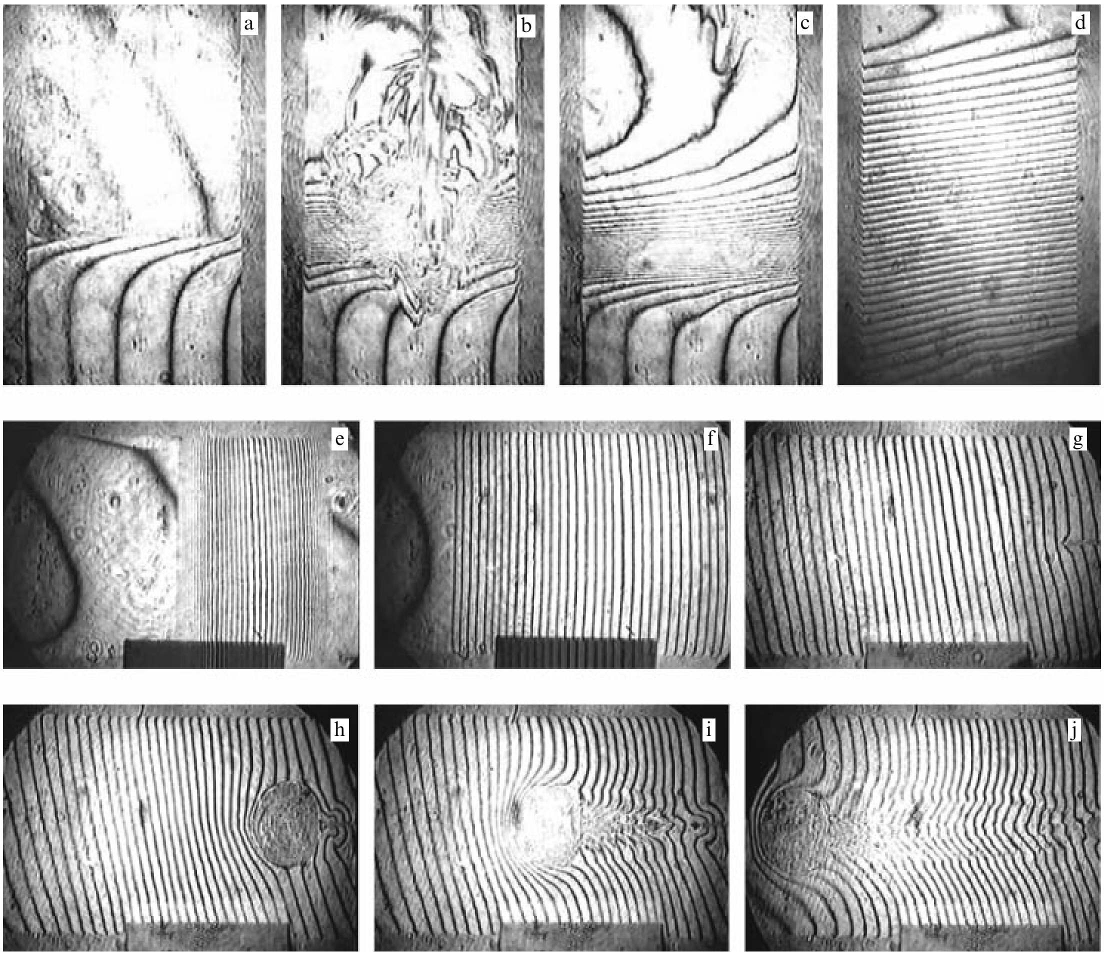

Figure 8. Interferograms of the concentration field of methyl alcohol in a cell. The dark rectangle below the bubble is a marker 3 cm in length.

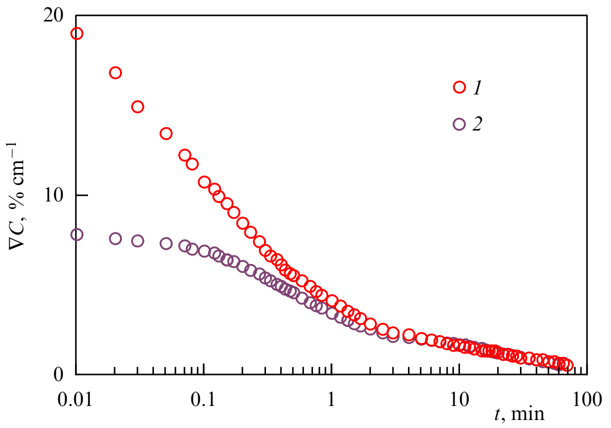

Figure 9. Time dependence of the lateral concentration gradient of methyl alcohol in the center of the container. The initial alcohol concentration C_0 in the solution: *1*, 80%; *2*, 90%.

alcohol was poured from above (Fig. 8b). In 10 – 20 s, a density-stratified concentration distribution settled in the cell under the action of the gravity force. It comprised two regions of the original liquids, one underlying the other one, separated by a thin diffusive transition zone (Fig. 8c). Owing to the smallness of the diffusion coefficient, this statically stable vertical concentration distribution could persist for several hours. The cell was then returned to the horizontal position. This created a strong lateral density contrast, which excited a convective shear flow in the system of liquids (Fig. 8e, f). The strength of this flow decayed rapidly with time because of the small layer thickness and vigorous mixing of the alcohol and its solution in oppositely directed flows. As a result, an extended region with a mild but almost homogeneous lateral gradient of concentration formed (Fig. 8g) in several minutes. The region was bounded by narrow zones of the original liquids in the vicinity of cell ends.

The dependence of the lateral concentration gradient on time at the center of the cell is presented in Fig. 9 in a logarithmic scale. A layer of pure methanol was poured over a solution with the concentration 80% in one case and 90% in the other. As can be seen, already 1 min after the liquids started to spread, the gradient curves practically matched each other despite the 10% difference in the initial concentrations. In both cases, the gradient first rapidly decreased to 2.5% cm^{-1} owing to the shear motion and then slowly decayed during a sufficiently long time interval (tens of minutes) of a nearly diffusive solution regime. The lateral distribution of concentration formed in this way remained rather stable. It is likely that the arising density jumps were already too small to excite an intense convective motion. This assumption is confirmed by the fact that when the container was returned to the vertical position, the density stratification created in the cell was preserved without changes (Fig. 8d). It is worth mentioning that equilibration of the quasistationary horizontal gradient of stratification occurs just because the thickness of the liquid layer is so small (~ 1 mm). In experiments with thicker cells (~ 2 mm and larger), the picture of convective flow was totally different: turning such cells (after they are filled) from the vertical to the horizontal position was accompanied by a flow of the lighter liquid over the denser one, creating a system of two thin horizontal layers located one over the other and essentially differing in concentration. Therefore, the small thickness of the liquid layer seems to be a fundamental prerequisite of the successful experiment.

The quasistationary, close-to-linear horizontal gradient of methyl alcohol stratification created as described above was used to study solutocapillary migration of bubbles. For this, an air bubble was injected into the solution layer with a medical syringe. The bubble acquired the shape of a flat disk with the diameter d equal to 5 – 15 mm. As soon as the bubble was detached from the needle, it began to displace toward the higher concentration of alcohol (Fig. 8h – j). Simultaneous videorecording of the concentration field and the position of the bubble within it permitted determining the concentration gradient, the size of the bubble, and its speed at different time instants. The measurement accuracy amounted to 0.1% for the concentration, 0.01 mm for the diameter of the bubble, and 0.01 mm s^{-1} for the speed of the bubble. The relative error of the speed measurement did not exceed 5%. The horizontality of the cell was monitored with an optical quadrant to an accuracy of 0.01°.

3.4 Bubble migration speed

Our experiments show that similarly to the case of thermocapillary migration [62], the speed of solutocapillary motion is directly proportional to the surface tension gradient and the diameter of the bubble. The results of experiments conducted with bubbles of different sizes and for different values of the concentration gradient ∇C are displayed in Fig. 10 (line *1*). Here, the abscissa presents the quantity

$$U = \frac{R}{\eta}\,\Delta\sigma = \frac{R}{\eta}\,\frac{\partial\sigma}{\partial C}\,\Delta C\,,$$

which was chosen, as in Ref. [55], as a unit of the solutocapillary migration speed. For comparison, the same plot presents the thermocapillary migration speed measured for air bubbles in methanol (line *2*) using the technique in Ref. [62]. In this case, the unit for the thermocapillary migration speed is

$$U = \frac{R}{\eta}\,\Delta\sigma = \frac{R}{\eta}\,\frac{\partial\sigma}{\partial T}\,\Delta T\,,$$

where R is the horizontal radius of the bubble and ΔC and ΔT are jumps in the surfactant concentration and the tempera-

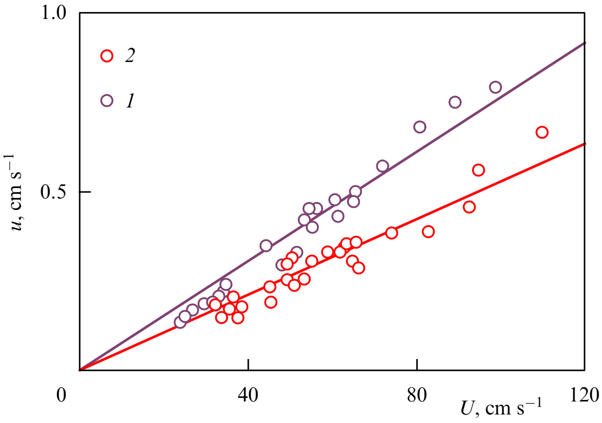

Figure 10. Velocity of bubble motion: *1*, solutocapillary migration (methanol); *2*, thermocapillary migration (ethanol).

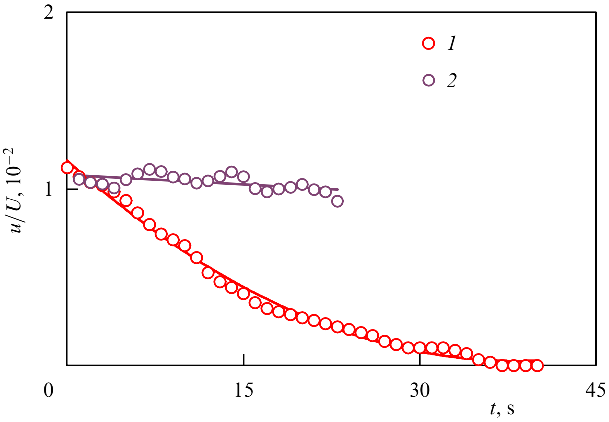

Figure 11. Velocity of bubble motion as a function of time: *1*, solutocapillary migration (methanol, bubble diameter $d = 7$ mm, and concentration gradient $\nabla C = 2.5\%$ cm^{-1}); *2*, thermocapillary migration (methanol, bubble diameter $d = 4.2$ mm, and temperature gradient $\nabla T = 3.5\,^{\circ}\mathrm{C\,cm^{-1}}$).

ture at opposite (in the direction of motion) poles of the bubble. Both dependences show a good linear behavior, but the absolute values in the thermocapillary case appear larger by almost a factor of 1.5 than in the solutocapillary case. The reason for this discrepancy is that the speed of solutocapillary migration did not stay constant and decreased with time, and hence the amplitudes presented in Fig. 10 were somewhat lower because of averaging over the measurement interval (which was ~ 10 s).

The dependence of the bubble migration speed on time is plotted in Fig. 11. Here, the ordinate axis corresponds to the migration speed in velocity units. It can be seen that while the bubble moved with a constant speed independent of time in the homogeneous temperature gradient (line *2*), the migration velocity monotonically decreased to zero over $\sim 40-60$ s (line *1*) in the solutal case. This happened even when a significant stratification gradient remained in the solution surrounding the bubble. But a new bubble introduced in the vicinity of a bubble that had come to rest nevertheless began to move. On changing the size of the bubble, the behavior was preserved qualitatively, but the time of motion and the path length increased with an increase in the diameter. To explain the reduction in speed, we can assume that saturation of the bubble surface by alcohol occurred through absorption from the solution. The surfactant diffusion in the bulk was insufficient to fully counteract the absorption and the buildup of a uniform distribution at the free surface and in its vicinity. As a result, the surface tension on the surface of the bubble became uniform relatively fast, independently of the magnitude of the concentration gradient in the ambient fluid, extinguishing the driving force.

4. Oscillatory regimes of solutal convection

4.1 Thermocapillary flow around air bubbles

The results of many investigations [72–81] show that if an upward-directed temperature gradient is maintained in a liquid, a thermocapillary flow forms around a bubble pressed against the underlying rigid surface in the form of an axisymmetric torus-like vortex with a vertical symmetry axis. Under the action of Marangoni forces, the liquid flows along the bubble-free surface to its lower pole and slowly rises at some distance, creating a returning flow. Correspondingly, in any vertical plane drawn through a diameter, two stationary vortices that are symmetric with respect to the bubble are observed. The temperature distribution also remains stationary. The flow stays stable up to the Marangoni numbers $\sim 3 \times 10^4$ [74, 76, 78], when it becomes three-dimensional, acquiring an azimuthal velocity component. As a result, a weak and slow oscillation of the temperature field develops near the bubble in the horizontal plane, while the toroidal vortex itself begins to vacillate, displacing repeatedly to the right and left relative to the center of the bubble [78]. The excitation of this oscillatory mode is independent of the gravitational force [80], and although the nature of this phenomenon is still debatable, it can likely be attributed to the ordinary loss of stability of the laminar flow at high motion speeds. The mere structure of the thermocapillary flow in the vertical plain (a stationary vortex) is preserved in this case.

4.2 Behavior of air bubbles in a two-layer system of liquids

The situation with a bubble placed in an extended horizontal liquid layer with a vertical jump in the surfactant concentration unfolds in a different way [82–86]. To create this gradient, the experimental cell described in Section 3.3 was used, but with the larger thickness 2.6 mm. Similarly, the cell was successively filled in an upright position with two miscible liquids. After the cell was returned from the vertical to the horizontal position, the lighter layer flowed over the denser one, forming a two-layer system with a vertical stratification in concentration. Experiments were conducted with water and aqueous solutions of various surfactants: acetic acid with concentrations ranging from 0 to 70%, and methyl, isopropyl, and ethyl alcohols with concentrations 50–100%. Noteworthy, the density of acetic acid is higher than that of water, but the density of alcohols is lower. In this way, variants with the surfactant layer located both above and below the water layer were implemented, allowing upward and downward directions of the surface tension gradient formed over the surface of the bubble. For the horizontal placement of the cell, the propagation direction and the density gradient of the unperturbed system of liquids were aligned, and the interference pattern was monotonic (there was no difference in optical paths). On injecting a cylindrical air bubble (with the diameter larger than the layer thickness) into the cell cavity, a Marangoni flow must form tangent to its surface. Driven by solutocapillary forces, it is to transfer the surfactant toward the lower (in experiments with methyl alcohol) or upper (in experiments with acetic acid) parts of the surface of the bubble.

By analogy with the thermocapillary convection, it could be expected that the emerging flow would be stationary. The approaching lighter or denser liquid fraction has to partly dissolve in the ambient liquid and partly return (ascend or sink, respectively), creating a steady convective flow in the form of an axisymmetric vertical vortex. But it turned out that the unfolding convection had a clearly expressed oscillatory character. Its development is illustrated by a series of interferograms in Fig. 12. Immediately after injecting the bubble, no flow was observed in the surrounding liquid and the concentration field around it stayed intact (Fig. 12a). Suddenly, a system of circular concentration isolines appeared (Fig. 12b). This was the result of an abrupt injection into the surrounding solution of an excessive

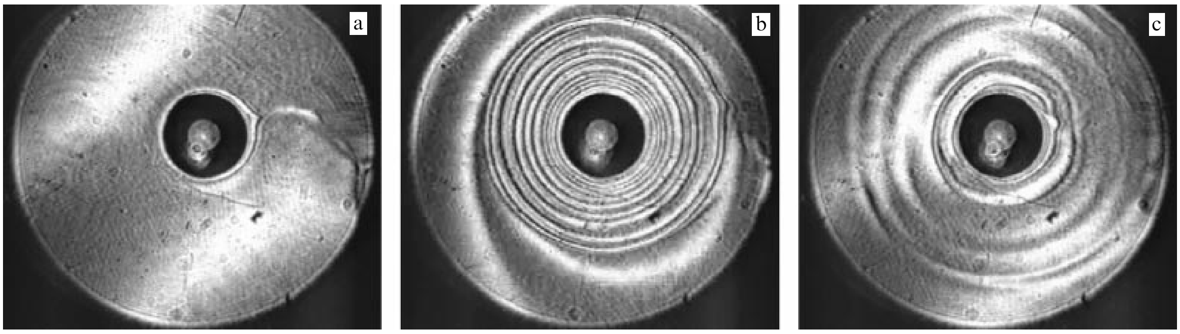

$t = 0$ s $t = 2.0$ s $t = 10$ s

Figure 12. Evolution of a perturbation of the concentration field around an air bubble in a horizontal layer of water solution of isopropyl alcohol (a view from above). The layer thickness h = 2.6 mm, the difference of concentrations ΔC = 20%, and the bubble diameter d = 5.0 mm.

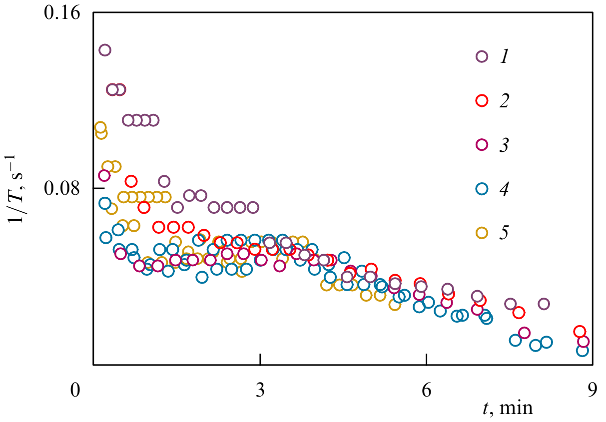

Figure 13. Time dependence of the oscillation frequency for bubbles of diameter d, mm: 15.0 (*1*), 10.7 (*2*), 7.1 (*3*), 5.1 (*4*). and 2.4 (*5*) in a two-layer system of liquids consisting of a 40% solution of acetic acid and water.

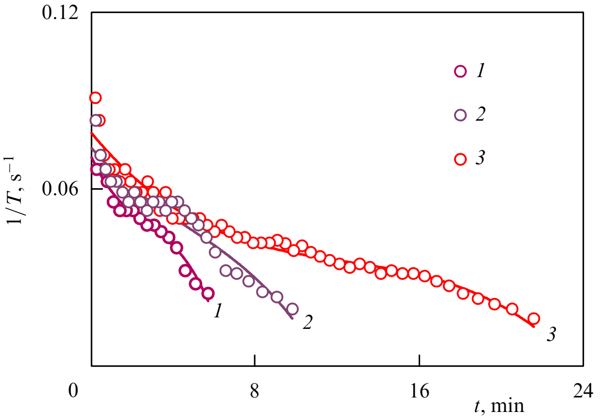

Figure 14. Time dependence of the oscillation frequency in a two-layer system of liquids consisting of an acetic acid solution and water. The diameter of bubbles $d = 4.8-5.9$ mm. The initial difference of the concentrations ΔC is 20% (curve *1*), 40% (curve *2*), and 70% (curve *3*).

amount of the surfactant accumulated under the action of solutocapillary forces respectively in the lower or upper part of the surface of the bubble. Subsequently, as the Archimedes force regenerated a vertical density stratification of the solution, the perturbation of the concentration field disappeared (Fig. 12c) and the interference pattern returned to a monotonic one.

This process occurred repeatedly with a good periodicity until the liquid surrounding the bubble was uniformly mixed. The period of this oscillation (the time interval between subsequent outbreaks of strong convection) was confined between a few seconds and minutes and was a function of time, the layer thickness, the horizontal bubble diameter, the initial concentration difference, and the properties of the liquids. Figure 13 presents the time dependence of the oscillation frequency for bubbles 2.4 – 15 mm in diameter in a two-layer system consisting of a 40% solution of acetic acid and water. Apparently, as the solution is mixed and the vertical stratification is reduced, the period of oscillations, initially equal to 10 s, gradually increases (and the oscillation frequency decreases accordingly) and the oscillations take longer and longer and totally stop in approximately 10 min. No significant dependence of the oscillation frequency on the bubble size was observed; the frequency only slightly decreased with a reduction in the bubble size and, additionally, smaller bubbles came to rest somewhat earlier. The oscillation frequency was actually determined by the layer thickness (i.e., the vertical bubble size) and the concentration gradient. On increasing the layer thickness or decreasing the initial difference in concentrations (Fig. 14), the oscillation period slightly increased. But the duration (the lifetime) of oscillations increased rather strongly with an increase in the initial concentration difference. A characteristic feature of all observed oscillations was, however, that they all disappeared abruptly: the oscillations of the concentration field near the bubble persisted with a decreasing period over a long time interval and then died out despite some vertical concentration gradient still existing.

To the largest extent, this phenomenon proved to be dependent on the choice of the surfactant and the range of its concentrations. In experiments with water and 15 – 60% solutions of acetic acid, well expressed oscillations were observed, characterized by a large period (tens of seconds and longer). For low surfactant concentrations, the oscillations never occurred; for high concentrations (in excess of 60%), they occurred so frequently that they merged into a continuous 'boiling' of the saturated surfactant solution near the bubble. In experiments with alcohol solutions, in contrast, the range of concentrations supporting the oscillations was narrower, and 'boiling' was the dominating regime of mass exchange. Obviously, the period and duration of oscillations are in reality determined not so much by the difference in concentrations as by the respective difference in surface tensions, which nonlinearly depends on the concentration for most solutions. Indeed, for the system of liquids consisting of two solutions of acetic acid (40% and 70%), the surfactant transfer occurred more slowly than in experiments with water and a 30% solution of acetic acid (i.e., with the same initial difference in the surfactant concentration) because of a smaller difference of surface tensions of the solutions. As a result, the period increased up to values of several minutes and the oscillations sometimes lasted for several hours.

The experimental findings reveal that the generation of solutocapillary flows has a threshold character because critical values must be achieved by some parameters determined by both the problem geometry and the physical characteristics of liquids (mostly by surface tension, but also density and viscosity). The nonstationary character of the solutocapillary Marangoni convection, periodically 'flaring' up and then decaying, could be a consequence of the interaction (competition) of two different mechanisms of convective mass transfer. The first would be the intensive Marangoni convection transporting the surfactant tangent to a bubble-free surface and quickly decaying because the surface concentration of the surfactant equalized owing to mixing in the solution near the bubble. The second mechanism is conditioned by the action of Archimedes forces through the formation of a relatively slow global circulation in the cavity volume because of an upward motion of the solution with a high surfactant concentration. This circulation reestablishes the solution stratification destroyed near the surface of the bubble, and an intense capillary flow bursts again.

Unfortunately, such an experimental setup combining the vertical direction of observation (a view from above) and the horizontal orientation of the liquid layer did not permit us to directly explore the structure of convective flows and follow the evolution of the vertical surfactant concentration distribution in the liquid.

4.3 Solutal flow near the surface of a bubble in a plane rectangular channel

4.3.1 Experimental technique. Further research [87–89] dealt with air bubbles placed into an elongated horizontal channel with a rectangular cross section. The choice of this geometry for the working cavity, on the one hand, permitted obtaining a peculiar vertical slab analog of the horizontal layer of a stratified fluid with a bubble inside, and, on the other hand, opened prospects for comparing experimental results with those of simulations of the Marangoni convection in the vicinity of a free surface in a rectangular domain (in a two-dimensional setup). In the experiments, a liquid filled a narrow clearance between two vertical glass plates with a semitransparent reflecting coating (a vertically positioned Hele–Shaw cell), inside which a horizontal channel 2 mm in height and 1.2 mm in width was formed by two inserts placed from above and from below. Owing to the smallness of the clearance width, the emerging flows and concentration fields could be treated as two-dimensional.

The experiments were conducted with various initial concentration distributions of surfactants, with aqueous solutions of methyl, ethyl, and isopropyl alcohols having been selected. Solutions of methyl alcohol have the smallest viscosity and solutal coefficient of surface tension, while isopropyl alcohol has the largest. The diffusion coefficients are, in contrast, maximal for methyl alcohol solutions and minimal for isopropyl alcohol solutions. The densities of all alcohols are close to each other. As a consequence, a wide range of liquid parameters and dimensionless Marangoni and Grashof diffusion numbers was covered by the experiments.

A horizontal light beam passed through a channel in a Fizeau interferometer allows visualizing the surfactant concentration field in a vertical section as a system of isolines of the refractive index. The difference of the refractive index values between two neighboring monotonic interference fringes computed for the given channel width was 0.27×10^{-3}. With due account for the nonlinear shape of the solutal dependence of the refractive index, this translates into an anomaly in the surfactant concentration of approximately 0.33–0.35%, 0.38–0.53%, and 1.10–1.33% for isopropyl, ethyl, and methyl alcohols, respectively. The error in measuring the concentration did not exceed 0.05%.

In the first set of experiments, the channel was initially filled with distilled water or a homogeneous solution of alcohol with the concentration 1–10%. A bubble was injected with a medical syringe at one of the channel ends such that it fully closed the channel, with only one free side surface. Then, a higher-concentration (up to 40%) and therefore lighter alcohol solution was gradually added from the other end, simultaneously with pumping out the excess liquid from the lower part of the channel. Because of the difference in densities, a relatively slow large-scale gravity current occurred in the channel, exhibiting a narrow tongue of the higher-concentrated surfactant solution flowing near the upper surface of the channel toward the bubble surface and forming a region with an upward directed concentration gradient in its vicinity. The magnitude of the gradient was set by the velocity and concentration of the approaching surfactant flow and by the initial concentration of the solution filling the channel.

In the second set of experiments, a vertical stratification in the surfactant concentration was initially created in the channel, and then an air bubble was injected. With this technique, much higher initial concentration gradients and, correspondingly, concentration-based Marangoni numbers were achieved, which, to a high degree, determined the intensity and duration of emerging oscillations.

4.3.2 The structure of convective flow. Figure 15 presents interferograms of the concentration field in the vicinity of the side boundary of an air bubble in a solution of isopropyl alcohol. It was found that in contrast to the thermocapillary case, the solutocapillary flow sets not immediately after the bubble surface is reached by the surfactant tongue but after some time (to be counted from the instant of contact between the tongue and the bubble surface). In the experiment with an air bubble in the solution of isopropyl alcohol (Fig. 15a, b), the time Δt that elapsed from the instant of contact between the surfactant and the surface to the instant of the appearance of a convective vortex (Fig. 15c) was 28 s, whereas the jump ΔC^* in concentration of the solution between the lower and upper parts of the bubble surface, caused by the continuing motion of the tongue, reached 2.2%. The equilibrium was then abruptly broken, and an intense Marangoni flow set in very fast, within approximately 0.2 s, which transported the surfactant tangent to the surface of the bubble at its lower part (Fig. 15d) under the action of capillary forces. This flow, by virtue of the continuity of the liquid, accelerated the supply of the more concentrated surfactant solution to the bubble surface along the upper surface of the cavity and, in this

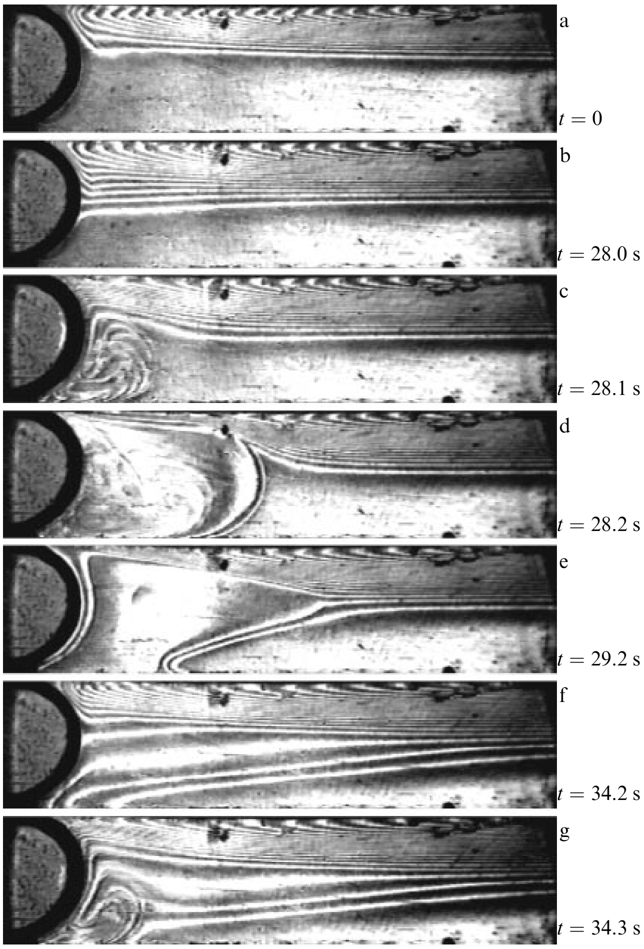

Figure 15. Interferograms of the concentration field of isopropyl alcohol in the vicinity of an air bubble in a channel in experiments with a surfactant tongue flowing to the bubble.

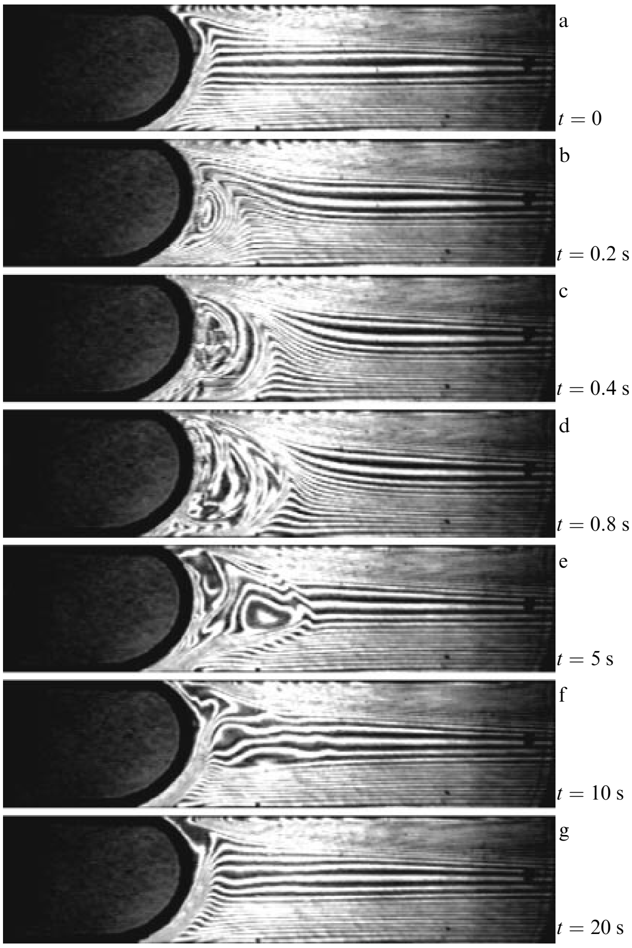

Figure 16. Interferograms of the concentration field of ethyl alcohol in the vicinity of an air bubble in a channel in experiments with an initial vertical surfactant stratification.

manner, strongly amplified the solutocapillary flow. This created a convective vortex. On its outer side, the liquid that had been entrained by the Marangoni flow near the bubble surface rose, driven by Archimedes forces in a returning flow. Growing and entraining more and more solution with a higher surfactant concentration, the vortex cell progressively became lighter and moved upward, finally cutting the flow rich in alcohol off the upper part of the surface of the bubble. The Marangoni flow ceased leaving the bubble surface, washed by a thin liquid layer of the same surfactant concentration.

However, the decay of the capillary flow did not imply that the liquid in the channel came to rest. Relaxation of the acquired horizontal gradient in the surfactant concentration is accompanied by a slow advective transport. By restoring the previously destroyed solutal stratification, it pulled the solution enriched in the surfactant to the upper part of the bubble. As the surfactant flow touched the bubble surface, a convective vortex reappeared (Fig. 15f, g). The cycle was repeated many times, but the period of oscillations increased with time while the intensity of the vortex flow decreased. This happened because of a gradual decrease in the gradient of the solution vertical stratification related to convective mixing. The Marangoni convection terminated when the concentration equalized almost completely. Interestingly, after the very first cycle, the development of capillary motion in all subsequent cycles began at much smaller jumps in the concentration along the bubble surface (Fig. 15f, the beginning of the second cycle, $\Delta C^* \sim 0.6\%$). Simultaneously, the mean surfactant concentration at the surface of the bubble increased from cycle to cycle. This can serve as a plausible explanation for the observed significant decrease in the critical concentration difference between the top and the bottom of the bubble at the inception of following cycles of vortex convective motion.

Similar oscillations were also observed when the bubble was placed in a channel with a vertically stratified surfactant solution. The presence of a free surface destroyed the stable stratification of the concentration field. Typical interference patterns that allow visualizing the evolution of the concentration field near the bubble within a single period of oscillations are presented in Fig. 16 for ethyl alcohol. As follows from the interferograms, the unfolding of the Marangoni convection already occurs after several tenths of a second measured from the instant the bubble was injected into the solution, which is taken as the reference point (Fig. 16a, b). The convection originating in this case turned out to be so vigorous that it destroyed the vertical surfactant stratification within a time interval less than 1 s (Fig. 16c, d), thus suppressing the capillary motion. The liquid of uniform density formed due to convective mixing was then pushed out from the bubble surface into the middle part of the channel by the advective flow (Fig. 16e, f). Gradually, the stratification close to the initial one was recovered near the boundary of the bubble (Fig. 16g), followed by the next burst of Marangoni convection. In this way, an oscillating flow was established with the initial period close to 20 s.

4.3.3 Threshold for the occurrence of solutocapillary stresses. The delay observed in the onset of Marangoni convection might be related to the formation of a surfactant surface phase that controls the transition of solute between phases. It is commonly assumed that the emergence of the surface phase proceeds in two stages. Surfactant molecules reach the interface via diffusive transport because the normal component of the convective velocity is zero at the boundary as a consequence of impermeability. The surface phase proper then forms via absorption and desorption processes. In experiments with the surfactant tongue advancing to the bubble, the delay Δt in the Marangoni convection can be measured from several tens of seconds to minutes depending on the velocity of the surfactant inflow. A scatter that large occurs, seemingly, because the time interval Δt is the combination of two intervals. The first is the time it takes the surfactant molecules to penetrate several molecular layers of water near the free surface in the diffusive regime. The second interval is the time it takes an initial 'seed' of the new surface phase, needed for the formation of a surface tension gradient, to occur. Exploring the dependence of the critical Marangoni number

$$\mathrm{Ma}^* = \frac{h}{\eta D}\frac{\partial\sigma}{\partial C}\,\Delta C^*$$

(determined by the maximum difference of concentrations between the upper and lower boundaries of the bubble at the onset of intensive convection) on the time interval between the contact of the surfactant with the surface of the bubble and vortex formation showed that prior to the burst of capillary convection, a large concentration gradient arose in the case of large flow velocities owing to diffusive time scale of the transfer of surfactant molecules to the surface. On the other hand, at small flow velocities (for Δt in excess of 1 min), the main role is played by the process through which a certain surface concentration is achieved, and hence critical values of the Marangoni number Ma^* are nearly equal for different flow velocities and surfactants.

The dependence of the critical Marangoni numbers corresponding to the instant when the first vortex developed on the initial surfactant content in the solution surrounding the bubble was explored in special experiments [89]. For this, homogeneous alcohol solutions of various initial concentrations C_0 were used instead of pure water to fill a channel. It turned out that as C_0 increases, the values of Ma^* monotonically decrease. Because an increase in the surfactant concentration in the solution leads primarily to a decrease in the surface tension coefficient σ at its free surface, an apparent correlation is observed between critical Marangoni numbers and the values of σ. Thus, the release of a surfactant from the solution to the interface between phases becomes essentially easier as the interfacial tension is reduced. Molecules of pure water, which have the maximum surface tension (72 mN m^{-1}), turn out to be so densely packed and strongly bonded to each other at the free surface that they imitate an elastic wall for the impinging surfactant flow. The result is the deformation of the flow and spreading around the interface between phases without outcropping to the surface. The surfactant molecules then tunnel through the boundary molecular barrier in a purely diffusive regime. A Marangoni flow begins upon an increase in the external surfactant gradient when a local excess in surfactant molecules is created over the upper part of the boundary of a bubble making contact with a more concentrated solution and the equilibrium of capillary forces can no longer be sustained. The mean concentration of alcohol at the surface increases with time, which reduces the surface tension, and the development of the capillary motion is already possible for much smaller jumps in concentration.

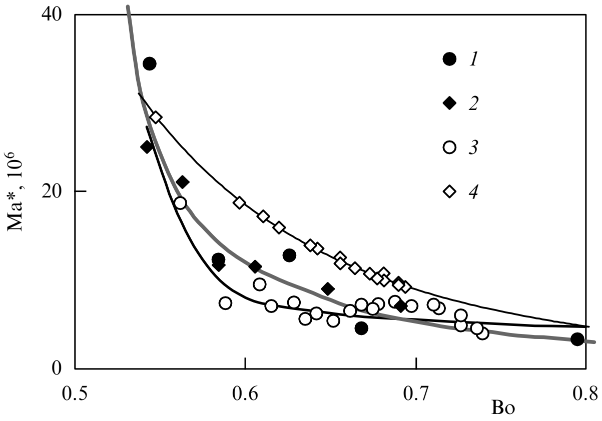

Figure 17. Dependence of the critical Marangoni number on the Bond number for bubbles in surfactant solutions of various concentrations (*1*, ethanol; *2*, isopropanol) and at the instant the intense convection cycles begin (*3*, ethanol; *4*, isopropanol).

Figure 17 plots the behavior of the critical Marangoni number at the onset of different cycles of vortex flow in solutions of ethanol and isopropanol (points *1* and *2*) as a function of the Bond number $\mathrm{Bo} = \rho g h^2/\sigma$ characterizing the intensity of capillary forces at the surface. The Bond numbers involve values of surface tension coefficients corresponding to the mean surfactant concentration at the surface of air bubbles at the instants of intensified motion. Also plotted are the measurement results for the dependence of Ma^* on Bo obtained in experiments with different initial concentrations of solutions (the solid lines fitted through points *3* and *4*). As can be seen, the values of Ma^* obtained in different experiments and conditions are fairly close in magnitude and demonstrate good agreement in the qualitative shape of all dependences.

4.3.4 Dynamics of the oscillation period. The temporal behavior of the oscillation period of the convective flow near a bubble has been studied experimentally in a channel filled with solutions of ethanol, isopropanol, and methanol with various initial concentration differences. The time was measured from the beginning of the first oscillation. In all cases, the oscillation frequency of the flow near the bubble surface was rather high initially (and the period T, accordingly, was small: $\sim 5-10$ s). The period then monotonically increased with time, and the oscillations abruptly ceased after some time interval. We note that in experiments with isopropanol solutions of a higher initial concentration ($C_0 = 40\%$), the oscillation frequency was lower and the oscillations themselves ceased significantly earlier than in experiments with solutions of a lower concentration ($C_0 = 20\%$). This is a consequence of the circumstance that despite the approximately equal concentrations differences between the upper and lower boundaries of the channel in both cases, the mean concentrations of solution in the vicinity of the bubble was different, and the contrast in the surface tension at its surface turned out to be larger in the second case owing to the nonlinear dependence of the alcohol surface tension coefficient on its concentration. Accordingly, the values of solutal Marangoni numbers Ma were higher, which implied that the solutocapillary convection was more intense and persisted longer. The results obtained in these studies agree well with observational data [82, 83] for solutal convection near a bubble in a horizontal layer with a vertical surfactant gradient, which show a similar temporal behavior of the oscillation period.

The experimental data reveal that at the initial stage at least, the oscillation frequency is to a large extent determined by the surface tension gradient at the surface of a bubble (depending, in turn, on the mean concentration of the solution and the difference in concentration between the lower and upper boundaries of the liquid layer). Then, after a relatively short process of mixing in the initially inhomogeneous solution, a large-scale advective flow driven by a lateral difference in the solution density is established in the channel. The oscillation period at this stage is determined by the intensity of the flow supplying new portions of the surfactant to the surface of the bubble and in this way triggering a vortical Marangoni flow. Therefore, the time between the burst and the decay of the vortex cell was approximately 0.3 of the whole oscillation period in the first oscillatory cycles, but this fraction reduced to 0.1 and remained nearly constant in the subsequent evolution.

The explanation for the increase in the oscillation period with time lies in a gradual convective mixing of the solution, owing to which the mean concentration of the surfactant in the channel increases and the vertical contrast in concentration decreases. This entails the reduction in the effective Marangoni and Grashof numbers

$$\mathrm{Gr} = \frac{gh^3}{\rho\nu^2}\frac{\partial\rho}{\partial C}\,\Delta C$$

where ν is the kinematic viscosity of the solution. The Grashof number was determined by the difference in the alcohol concentration at the upper and lower channel boundaries sufficiently far from the bubble surface (at the distance equal to three layer thicknesses), where the perturbations of the vertical concentration gradient due to the Marangoni convection in the vicinity of the bubble were absent. Time dependences of the period of convective oscillations and the respective Grashof numbers found in experiments with various alcohols are presented in Figs 18 and 19 in a dimensionless form. The viscous time $\tau = h^2/\nu$ is used as a time unit.

The collected experimental data were compared to the results of numerical simulations in Ref. [88]. In that work, a convection model with a diffusive transport of the surfactant to the bubble surface was used (without account for the formation of a surface phase). A rectangular cavity elongated in the horizontal direction was considered. One of its vertical walls modeled the bubble surface impermeable for the surfactant. An initial horizontal gradient of the surfactant concentration was prescribed in the cavity. The simulations showed that at large Schmidt numbers $\mathrm{Sc} = \nu/D$ ($\sim 10^3$), self-sustained oscillating regimes of solutal flows could set in. In the background of a slow gravitational convection, short bursts of an order-of-magnitude stronger Marangoni convection were observed. The experiment and numerical simulation agree reasonably well as regards the pattern of convective motion and the oscillation period. The period of self-oscillations decreases with an increase in the Grashof number and is only weakly sensitive to the Marangoni number. The dependence of the period of established oscillations on the Grashof number is presented in Fig. 20. Points *1–4* in the plot correspond to experimental results obtained with various alcohols. The solid line corresponds to simulations at $\mathrm{Ma} = 10^6$ and $\mathrm{Sc} = 10^3$.

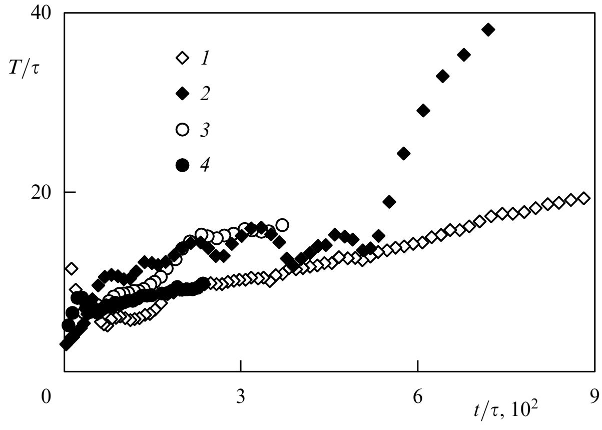

Figure 18. Time dependence of the oscillation period (in a dimensionless form) in experiments with isopropanol (*1*, *2*), ethanol (*3*), and methanol (*4*). Points *1* and *2–4* respectively correspond to the cases of a surfactant tongue flowing to the bubble and the initial linear concentration gradient.

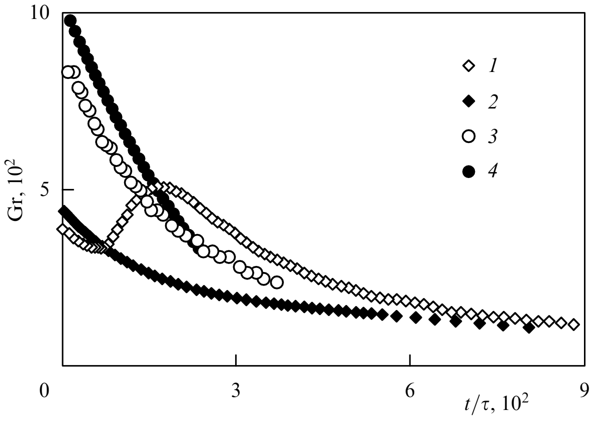

Figure 19. Dependence of the Grashof number on a dimensionless time in experiments with isopropanol (*1*, *2*), ethanol (*3*), and methanol (*4*). Points *1* and *2–4* respectively correspond to the cases of a surfactant tongue flowing to the bubble and the initial linear concentration gradient.

5. Conclusion

The experiments reviewed here demonstrate that an intensive solutal Marangoni convection develops along free surfaces of solutions characterized by a nonuniform distribution of the surfactant concentration. The flows and phenomena occurring in this case are in many respects similar to those of a thermocapillary origin and demonstrate similar behavior (in particular, the intensity is proportional to the surface tension gradient). At the same time, the solutocapillary phenomena exhibit some specific features related to the much larger

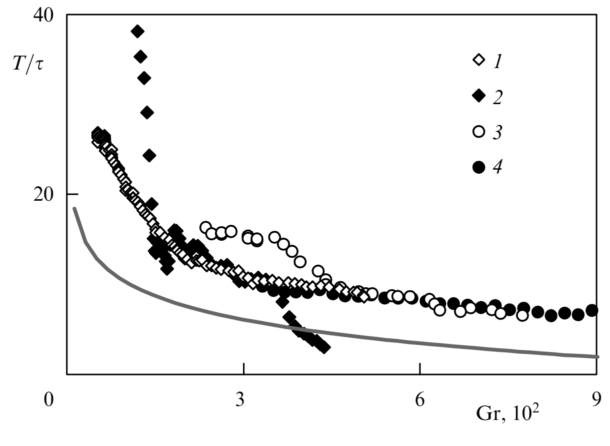

Figure 20. Dependence of the dimensionless oscillation period on the Grashof number in experiments with isopropanol (*1*, *2*), ethanol (*3*), and methanol (*4*). Points *1* and *2–4* respectively correspond to the cases of a surfactant tongue flowing to the bubble and the initial linear concentration gradient. The solid line represents the results of numerical simulations in Ref. [88].

Marangoni numbers achievable in experiments and the complex character of the process of the surface tension gradient formation, which derives from a slower (compared to heat transfer) diffusive transport of molecules with a low surface tension coefficient to the interface and a concurrent absorption there. As a result, the solutocapillary convection shows a markedly nonstationary behavior. The understanding of this distinct feature is necessary for constructing theoretical models of boundary conditions at the interface between phases, with proper account for the formation of the new, surface phase of the surfactant.

The experimental confirmation of the possibility of solutal migration of gas bubbles, clarification of the nature of the flows developing close to resting gaseous inclusions in inhomogeneous surfactant solutions, and the discovery of a threshold for the excitation of solutocapillary motion allow explaining many aspects of mass exchange and material structure formation in a number of technological experiments in microgravity, and predicting the behavior of complex systems of liquids and multiphase media in thin channels and layers, and in cavities of complex geometry. The results obtained in the experiments can be used in designing systems of passive homogenization in liquids and in optimizing working regimes of the already operational technology lines in various branches of industry. A special role can be played by the Marangoni effects elaborated here in the design of microsystems for cooling and heat exchange with multicomponent mixtures of liquids as a heat agent.

This work was supported by the Russian Foundation for Basic Research, projects No. 06-01-00221, RFBR-Ural No. 077-01-96031 and No. 07-01-96053.

References

1. Levich V G *Fiziko-khimicheskaya Gidrodinamika* (Physicochemical Hydrodynamics) 2nd ed. (Moscow: GIFML, 1959) [Translated into English (Englewood Cliffs, NJ: Prentice-Hall, 1962)]
2. Levich V G, Krylov V S *Annu. Rev. Fluid Mech.* **1** 293 (1969)
3. Scriven L E, Sternling C V *Nature* **187** 186 (1960)
4. Marangoni C *Sull'espansione delle gocce di un liquido gallegianti sulla superficie di altro liquido* (Pavia: Tipografia dei fratelli Fusi, 1865)
5. Vargaftik N B *Spravochnik po Teplofizicheskim Svoistvam Gazov i Zhidkostei* (Tables on the Thermophysical Properties of Liquids and Gases) 2nd ed. (Moscow: Nauka, 1972) [Translated into English (Washington: Hemisphere Publ. Corp., 1975)]
6. Nikol'skii B P (Ed.-in-Chief) *Spravochnik Khimika* (Handbook of Chemist) Vol. 3, 2nd ed. (Leningrad: Khimiya, 1964)
7. Abramzon A A, Shchukin E D (Eds) *Poverkhnostnye Yavleniya i Poverkhnostno-aktivnye Veshchestva*: Spravochnik (Surface Phenomena and Surface-Active Agents. Handbook) (Leningrad: Khimiya, 1984)
8. Berg J C, Acrivos A, Boudart Û *Adv. Chem. Eng.* **6** 61 (1966)
9. Fedorov K N, Ginzburg A I *Pripoverkhnostnyi Sloi Okeana* (Ocean Surface Layer) (Leningrad: Gidrometeoizdat, 1988)
10. Shapiro D L, Notter R H (Eds) *Surfactant Replacement Therapy* (New York: A.R. Liss, 1989)
11. Hershey A V *Phys. Rev.* **56** 204 (1939)
12. Povitskii A S, Lyubin L Ya *Osnovy Dinamiki i Teplomassoobmena Zhidkostei i Gazov pri Nevesomosti* (Fundamentals of Dynamics an Heat and Mass Transfer in Liquids and Gases in Weightlessness) (Moscow: Mashinostroenie, 1972)
13. Ganiev R F, Lapchinskii V F *Problemy Mekhaniki v Kosmicheskoi Tekhnologii* (Problems of Mechanics in Space Technology) (Moscow: Mashinostroenie, 1978)
14. Avduevskii V S et al. *Problemy Kosmicheskogo Proizvodstva* (Problems of Space Technology) (Moscow: Mashinostroenie, 1980)
15. Grishin S D, Leskov L V *Industrializatsiya Kosmosa*: *Problemy i Perspektivy* (Industrialization of Space: Problems and Perspectives) (Moscow: Nauka, 1987)
16. Avduevskii V S, Polezhaev V I (Eds) *Gidromekhanika i Teplomassoobmen v Nevesomosti* (Fluid Dynamics and Heat and Mass Transfer in Weightlessness) (Moscow: Nauka, 1982)
17. Avduevskii V S (Ed.-in-Chief) *Gidromekhanika i Protsessy Perenosa v Nevesomosti* (Fluid Dynamics and Transfer Processes in Weightlessness) (Sverdlovsk: UNTs AN SSSR, 1983)
18. Avduevskii V S (Ed.-in-Chief) *Tekhnologicheskie Eksperimenty v Nevesomosti* (Technological Experiments in Weightlessness) (Sverdlovsk: UNTs AN SSSR, 1983)
19. Rath H J (Ed.) *Microgravity Fluid Mechanics* (Berlin: Springer-Verlag, 1992)
20. Monti R (Ed.) *Physics of Fluids in Microgravity* (London: Taylor & Francis, 2001)
21. Myshkis A D (Ed.) *Gidromekhanika Nevesomosti* (Low-Gravity Fluid Mechanics) (Moscow: Nauka, 1976) [Translated into English (Berlin: Springer-Verlag, 1987)]
22. Sanfeld A, Legros J C, Velarde M G, in *Fluid Sciences and Materials Science in Space*: *a European Perspective* (Ed. H U Walter) (Berlin: Springer-Verlag, 1987) p. 84
23. Birikh R V et al. *Liquid Interfacial Systems*: *Oscillations and Instability* (New York: Marcel Dekker, 2003)
24. Ostrach S, in *Materials Sciences in Space with Application to Space Processing* (Prog. in Astronautics and Aeronautics, Vol. 52, Ed. L Steg) (New York: Am. Inst. of Aeronautics and Astronautics, 1977) [Translated into Russian (Moscow: Mir, 1980) p. 9]
25. Abramzon A A *Poverkhnostno-aktivnye Veshchestva. Svoistva i Primenenie* (Surface-Active Substances. Properties and Applications) 2nd ed. (Leningrad: Khimiya, 1981)
26. Adamson A W *Physical Chemistry of Surfaces* 3rd ed. (New York: Wiley, 1976) [Translated into Russian (Moscow: Mir, 1979)]
27. Gaines G L (Jr.) *Insoluble Monolayers at Liquid-Gas Interfaces* (New-York: Wiley Intersci. Publ., 1966)
28. Palmer H J, Berg J C *J. Fluid Mech.* **47** 779 (1971)
29. Barton K D, Subramanian R S *J. Colloid Interface Sci.* **133** 211 (1989)
30. Chen J, Stebe K J *J. Fluid Mech.* **340** 35 (1997)
31. Palmer H J, Berg J C *J. Fluid Mech.* **51** 385 (1972)
32. Kamotani Y et al. *Int. J. Heat Mass Transfer* **28** 165 (1985)
33. Nallani M, Subramanian R S *J. Colloid Interface Sci.* **157** 24 (1993)
34. Chen Y S et al. *Int. J. Multiphase Flow* **23** 325 (1997)
35. Landau L D, Lifshitz E M *Gidrodinamika* (Fluid Mechanics) (Moscow: Nauka, 1986) p. 296 [Translated into English (Oxford: Pergamon Press, 1987)]
36. Loulergue J C *Thin Solid Films* **82** 61 (1981)

37. Pshenichnikov A F, Tokmenina A G *Izv. Akad. Nauk SSSR Mekh. Zhidk. Gaza* (3) 150 (1983) [*Fluid Dynamics* **18** 463 (1983)]
38. Zuev A L, Pshenichnikov A F *Prikl. Mekh. Tekh. Fiz.* (3) 90 (1987) [*J. Appl. Mech. Tech. Phys.* **28** 399 (1987)]
39. Bratukhin Yu K, Briskman V A, Zuev A L, Pshenichnikov A F, in *Gigromeknanika i Teplomassoobmen pri Poluchenii Materialov* (Fluid Dynamics and Heat and Mass Transfer by Material Production) (Eds V S Avduevskii, V I Polezhaev) (Moscow: Nauka, 1990) p. 273
40. Briskman V A et al., in *Proc. 1st Intern. Symp. on Microgravity Research & Applications in Physical Sciences and Biotechnology, Sorento, Italy, 2000* (ESA SP, 454, Ed. B Schürmann) (Noordwijk: ESA Publ. Division, 2001) p. 207
41. Zuev A L, in *Termo- i Kontsentratsionno-Kapillyarnye Effekty v Slozhnykh Sistemakh* (Thermo- and Solutocapillary Effects in Complex Systems) (Ekaterinburg: Inst. Mekhaniki Sploshnykh Sred UrO RAN, 2003) p. 56
42. Wang M, Ming N *Phys. Rev. A* **44** R7898 (1991)
43. Bull J L, Grotberg J B *Exp. Fluids* **34** 1 (2003)
44. Gaver D P, Grotberg J B *J. Fluid Mech.* **213** 127 (1990)
45. Jensen O E, Grotberg J B *J. Fluid Mech.* **240** 259 (1992)
46. Halpern D, Grotberg J B *J. Fluid Mech.* **237** 1 (1992)
47. Jensen O E, Grotberg J B *Phys. Fluids A* **5** 58 (1993)
48. Ahmad J, Hansen R S *J. Colloid Interface Sci.* **38** 601 (1972)
49. Gaver D P, Grotberg J B *J. Fluid Mech.* **235** 399 (1992)
50. Starov V M, de Ryck A, Velarde M G *J. Colloid Interface Sci.* **190** 104 (1997)
51. Zuev A L, in *Gidrodinamika* (Fluid Dynamics) Issue 16 (Perm': PGU, 2007) p. 64
52. Zuev A L *Kolloid. Zh.* **69** 315 (2007) [*Colloid. J.* **69** 286 (2007)]
53. Vazquez G, Alvarez E, Navaza J M *J. Chem. Eng. Data* **40** 611 (1995)
54. Young N O, Goldstein J S, Block M J *J. Fluid Mech.* **6** 350 (1959)
55. Bratukhin Yu K *Izv. Akad. Nauk SSSR Mekh. Zhidk. Gaza* (5) 156 (1975)
56. Wozniak G, Siekman J, Srulijes J *Z. Flugwiss Weltraumforsch* **12** 137 (1988)
57. Chhabra R P, De Kee D (Eds) *Transport Processes in Bubbles, Drops, and Particles* (New York: Hemisphere Publ. Corp., 1992)
58. Subramanian R S, Balasubramaniam R *The Motion of Bubbles and Drops in Reduced Gravity* (Cambridge: Cambridge Univ. Press, 2001)
59. Subramanian R S, Balasubramaniam R, Wozniak G, in *Physics of Fluids in Microgravity* (Ed. R Monti) (London: Taylor & Francis, 2001) p. 149
60. Hardy S C *J. Colloid Interface Sci.* **69** 157 (1979)
61. Merritt R M, Subramanian R S *J. Colloid Interface Sci.* **125** 333 (1988)
62. Bratukhin Yu K, Zuev A L *Izv. Akad. Nauk SSSR Mekh. Zhidk. Gaza* (3) 62 (1984)
63. Bratukhin Yu K, Briskman V A, Viviani A, Zuev A L, AIAA Paper No. 2001-0763 (2001)
64. Mukai K, Lin W *Tetsu-to Hagané* **80** 527 (1994)
65. Mukai K, Lin W *Tetsu-to Hagané* **80** 533 (1994)
66. Wang Z, Mukai K, Lee I J *Iron. Steel Inst. Jpn. Int.* **39** 553 (1999)
67. Saffman P G *J. Fluid Mech.* **22** 385 (1965)
68. Zuev A L, Kostarev K G, Shmyrov A V, in *Termo- i Kontsentratsionno-Kapillyarnye Effekty v Slozhnykh Sistemakh* (Thermo- and Solutocapillary Effects in Complex Systems) (Ekaterinburg: Inst. Mekhaniki Sploshnykh Sred UrO RAN, 2003) p. 77
69. Zuev A L, Kostarev K G *Dokl. Ross. Akad. Nauk* **399** 490 (2004) [*Dokl. Phys.* **49** 747 (2004)]
70. Bratukhin Yu K, Kostarev K G, Viviani A, Zuev A L *Exp. Fluids* **38** 594 (2005)
71. Gustafson S E, Kjellander R A E *Z. Naturforsch. A* **23** 242 (1968)
72. Raake D, Siekmann J, Chun Ch-H *Exp. Fluids* **7** 164 (1989)
73. Wozniak K, Wozniak G, Rösgen T *Exp. Fluids* **10** 12 (1990)
74. Chun Ch-H, Raake D, Hansmann G *Exp. Fluids* **11** 359 (1991)
75. Rashidnia N, Balasubramaniam R *Exp. Fluids* **11** 167 (1991)
76. Kassemi M, Rashidnia N *Phys. Fluids* **12** 3133 (2000)
77. Arlabosse P et al. *Heat Transfer Trans. ASME* **122** 66 (2000)
78. Betz J, Straub J *Heat Mass Transfer* **37** 215 (2001)
79. Wozniak G et al. *Exp. Fluids* **31** 84 (2001)
80. Reynard C, Santini R, Tadrist L *Exp. Fluids* **31** 440 (2001)
81. Reynard C, Santini R, Tadrist L *C.R. Mecanique* **331** 237 (2003)
82. Zuev A L, Kostarev K G, in *Konvektivnye Techeniya* (Convective Flows) Issue 1 (Perm': PGPU, 2003) p. 123
83. Kostarev K, Zuev A, Viviani A *C.R. Mecanique* **332** 1 (2004)
84. Zuev A L, Kostarev K G, in *Gidrodinamika* (Fluid Dynamics) Issue 14 (Perm': PGU, 2003) p. 88
85. Kostarev K G, Viviani A, Zuev A L *Appl. Mech. Trans. ASME* **73** (1) 66 (2006)
86. Zuev A L, Kostarev K G *Zh. Eksp. Teor. Fiz.* **130** 363 (2006) [*JETP* **103** 317 (2006)]
87. Zuev A L, Kostarev K G, in *Konvektivnye Techeniya* (Convective Flows) Issue 2 (Perm': PGPU, 2005) p. 198
88. Birikh R V, Zuev A L, Kostarev K G, Rudakov R N *Izv. Ross. Akad. Nauk Mekh. Zhidk. Gaza* (4) 30 (2006) [*Fluid Dynamics* **41** 514 (2006)]
89. Bushueva K A, Denisova M O, Zuev A L, Kostarev K G, in *Konvektivnye Techeniya* (Convective Flows) Issue 3 (Perm': PGPU, 2007) p. 139